EARTH SURFACE PROCESSES AND LANDFORMS
Earth Surf. Process. Landforms, (2020)

Published online in Wiley Online Library
(wileyonlinelibrary.com) DOI: 10.1002/esp.4962

Sand settling through bedform-generated turbulence in rivers

Brendan Yuill,[1]* Yushi Wang,[1] Mead Allison,[2] Ehab Meselhe[2] and Chris Esposito[1]
[1] The Water Institute of the Gulf, 1110 River Road S, Suite 200, Baton Rouge, LA 70802, USA
[2] Tulane University, 6823 St Charles Ave, New Orleans, LA 70118, USA

Received 28 April 2020; Revised 15 June 2020; Accepted 15 July 2020

*Correspondence to: Brendan Yuill, The Water Institute of the Gulf, 1110 River Road S, Suite 200, Baton Rouge, LA 70802, USA. E-mail: brendan.yuill@gmail.com

ESPL
Earth Surface Processes and Landforms

ABSTRACT: Fluvial bedforms generate a turbulent wake that can impact suspended-sediment settling in the passing flow. This impact has implications for local suspended-sediment transport, bedform stability, and channel evolution; however, it is typically not well-considered in geomorphologic models. Our study uses a three-dimensional OpenFOAM hydrodynamic and particle-tracking model to investigate how turbulence generated from bedforms and the channel bed influences medium sand-sized particle settling, in terms of the distribution of suspended particles within the flow field and particle-settling velocities. The model resolved the effect of an engineered bedform, which altered the flow field in a manner similar to a natural dune. The modelling scenarios alternated bed morphology and the simulation of turbulence, using detached eddy simulation (DES), to differentiate the influence of bedform-generated turbulence relative to that of turbulence generated from the channel bed. The bedform generated a turbulent wake that was composed of eddies with significant anisotropic properties. The eddies and, to a lesser degree, turbulence arising from velocity shear at the bed substantially reduced settling velocities relative to the settling velocities predicted in the absence of turbulence. The eddies tended to advect sediment particles in their primary direction, diffuse particles throughout the flow column, and reduced settling likely due to production of a positively skewed vertical-velocity fluctuation distribution. Study results suggest that the bedform wake has a significant impact on particle-settling behaviour (up to a 50% reduction in settling velocity) at a scale capable of modulating local suspended transport rates and bedform dynamics. © 2020 John Wiley & Sons, Ltd.

KEYWORDS: sediment settling; turbulence; bedforms; rivers; suspended sediment

Introduction

Fluvial bedforms, such as dunes, generate a wake with a turbulent intensity greater than the surrounding flow that may stretch distances many times the bedform length (Smith and McLean, 1977; Müller and Gyr, 1986; Lapointe, 1992; Kostaschuk and Church, 1993; Bennett and Best, 1995; Venditti and Bauer, 2005). The wake is generated from velocity shear between slow-moving flow located downstream of the bedform lee side and swifter flow passing over the bedform crest (Best, 2005). The ability for river flow to suspend bed sediment particles is dependent on the turbulent intensity of the ambient flow (Middleton and Southard, 1984; Raudkivi, 1998; van Rijn, 2007). As such, properties of particle suspension, that include the trajectory and velocity of the particles settling out of suspension, may be influenced by contact with the turbulent wake (Lapointe, 1992; Kostaschuk and Villard, 1999; Venditti and Bennett, 2000; Chang, 2004; Kwoll *et al.*, 2013; Khosronejad and Sotiropoulos, 2014). Figure 1 shows a schematic of these phenomena and illustrates an example of how they may impact a settling sediment particle. Theoretical studies (e.g. Murray, 1970; Stout *et al.*, 1995) suggest that isotrophic (non-directional) turbulence, on the scale that occurs in rivers, may generate a nonlinear drag effect that reduces the settling rate of sand-sized sediment particles. There has been less study of how anisotropic (directional) turbulence, such as occurs in bedform wakes, explicitly impacts particle settling; however, processes linked to anisotropic turbulence have been shown to play a dominant role in maintaining suspension of bed material (Zedler and Street, 2001; Marchioli *et al.*, 2006; Chang and Park, 2016; Davies and Thorne, 2016). Further, the influence of anisotropic turbulence structures, in the form of ‘sweeps’ and ‘bursts’ (Grass, 1971), on promoting the entrainment and near-bed transport of bed sediment has been well documented (McLean *et al.*, 1994; Nelson *et al.*, 1995; Schmeeckle, 2015).

Sediment settling has important implications for river geomorphology. The flux of suspended-bed sediment is dependent on the balance of sediment deposition due to particle settling relative to sediment entrainment from the channel bed (Raudkivi, 1998). Sediment settling in bedform fields has been shown to influence the dimensions and translation velocities of those bedforms (Hand and Bartberger, 1988; Bennett *et al.*, 1998; Parsons and Best, 2013; Naqshband *et al.*, 2014; Bradley and Venditti, 2019). Despite this importance, precise simulation of particle-settling processes is often neglected in geomorphic models in favour of assuming a singular particle-settling velocity, typically set as the still-water particle-settling velocity (van Rijn and Tan, 1985; Paola *et al.*, 2011). This assumption is generally considered valid because geomorphic models are often used to simulate

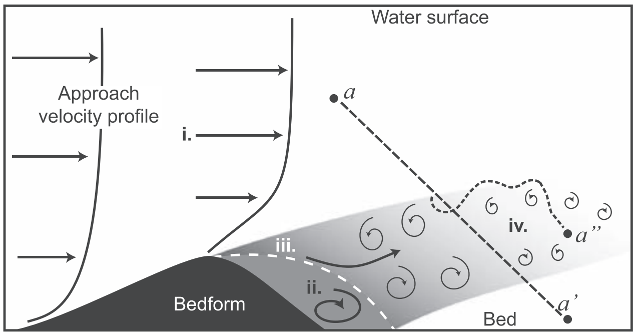

FIGURE 1. Schematic of a sediment particle settling through unidirectional flow over a bedform. In the schematic, the interface between (i) the swift flow passes over the bedform and (ii) the slower flow in the separation/recirculation zone near the bedform lee side produces (iii) an area of intense velocity shear. This velocity shear produces (iv) a turbulent wake. A hypothetical sediment particle at position *a* is settling through the flow column. In the absence of turbulence, the particle will settle with a relatively uniform trajectory (*a*–*a*′) based on the pull of gravity and currents. In the presence of turbulence, the particle trajectory is affected by chaotic upward and downward pulses of velocity associated with passing eddies and, while the average vertical velocity of the eddies may be negligible, the final particle trajectory (*a*–*a*″) and mean particle-settling rate may be significantly affected by the turbulence.

processes that operate at spatial and temporal scales much larger and longer than the hydrodynamic scales that influence particle settling (Howard, 1971; Johannesson and Parker, 1989; Murray and Paola, 1994; Nagata *et al.*, 2000; Duan and Julien, 2010). However, in studies where sub-channel reach sediment transport dynamics are of interest or where settling rates are highly variable, such as near bedform-generated wakes, typical geomorphic models may lead to poor replication of the active processes. A critical step in adding precision to geomorphic models in these situations requires a better understanding of how bedform-generated turbulence might modify sediment particle settling from that expected by the still-water settling properties or by reach-averaged flow properties. Identifying if bedform-generated turbulence generally increases or decreases settling rates, and at what relative magnitude this change might occur, would be instrumental in improving this understanding (Nielsen, 1993; Wang and Maxey, 1993; Chang and Park, 2016).

In this paper, we investigate the impact of bedform-generated turbulence on sediment particles settling in river-like flow conditions using numerical modelling. We focus our investigation on how the turbulent wake generated from a single, dune-scale bedform modifies the settling velocity of medium sand. Medium sand is a primary constituent of the bed material in many medium and large sandy rivers worldwide (Molinas and Wu, 2001). Our study employs a three-dimensional (3D) computation fluid dynamics (CFD) model that resolves turbulence using detached eddy simulation (DES) and particle settling using a Lagrangian particle-tracking solver. The objectives of our study include:

1 investigating how bedform-generated turbulence influences the velocity and suspended-particle fields in the local flow column;
2 quantifying the simulated impact of bedform-generated turbulence on sand-sized particle-settling velocities relative to those simulated over a flat channel bed and in the absence of resolved turbulence; and
3 based on the study results, discussing the implications of bedform-generated turbulence on suspended-bed sediment transport and bedform dynamics.

Methods

Overview

Our study methodology focused on the simulation of numerical model scenarios that systematically varied turbulence generation in river-like flow conditions. The objective of these scenarios was to identify the relative influence of turbulence generated from a large bedform and the channel bed on sand-sized particle settling, and to assess how this influence impacts suspended-sediment and bedform dynamics. We simulated bedform-generated turbulence by modelling the dynamic flow field over a single, fixed bedform. The bedform was based on a section of channel bed observed in the lower Mississippi River (USA) that was impacted from dredging. The dredging created a structure that had a lee-side slope with a length (20.6 m) and inclination (14°) analogous to a large natural dune (Figure 2). The lee-side slope was less than the angle of repose, which is consistent with the 'low-angle dune' bedform classification (Best, 2005).

Observed current-velocity profiling indicated that the engineered bedform impacted the local velocity field similar to a large natural dune (e.g. Parsons *et al.*, 2005; Kwoll *et al.*, 2013). Downstream of the bedform, mean velocities were significantly reduced while the mean velocity fluctuations were increased. Measurements of bed texture at the site found that the median grain-size diameter was 0.25 mm, which is typical for lower Mississippi River bars (Ramirez and Allison, 2013). Additional details about field data collected to characterize the modelled study site are available in the online Supporting Information.

The advantage of focusing the study on an engineered bedform is that a significant length of the bed upstream and downstream of the lee-side slope was relatively flat, so that the structure's impact on the flow and sediment transport could be isolated and identified. The majority of natural dunes develop in complex fields that contain multiple dunes of irregular size, shape, and orientation (e.g. Lapointe, 1992; Parsons *et al.*, 2005; Venditti and Bauer, 2005; Nittrouer *et al.*, 2008; Ramirez and Allison, 2013), which makes disentangling the hydrodynamic effect of an individual bedform property extremely difficult (Wren *et al.*, 2007). Past numerical and laboratory studies of bedform dynamics have adopted similar idealized approaches to simplify analyses and interpretation of results, such as by focusing on a singular structure (e.g. Nelson *et al.*, 1995; Grigoriadis *et al.*, 2009; Schmeeckle, 2015) or by employing idealized immobile, regularly spaced bedforms (e.g. McLean *et al.*, 1994; Venditti, 2007; Kwoll *et al.*, 2016).

In our model, spherical mass particles representing sediment grains were fed into suspension in unidirectionally flowing water and settled due to gravity. As the particles settled, we analysed the instantaneous and time-averaged vertical particle velocities, which we refer to as the 'vertical particle velocity' and the 'particle-settling velocity', respectively. In our study, we reference the terminal particle-settling velocity in still water, which we refer to as the 'still-water settling velocity'. The still-water settling velocity of a particle is an intrinsic geotechnical property of an individual sediment particle and is independent of the dynamics of surrounding fluid. Our analyses focused on the settling of a medium sand-sized particle (0.25 mm in diameter), with a density of 2650 kg m^{-3} and a terminal still-water fall velocity of 0.034 m s^{-1}. These sediment properties pertain to the approximate median particle size and density of lower Mississippi River sand bar sediment. The still-water fall velocity approximates that predicted using the empirical formula of Dietrich (1982): 0.031 m s^{-1}. In our study, while flow

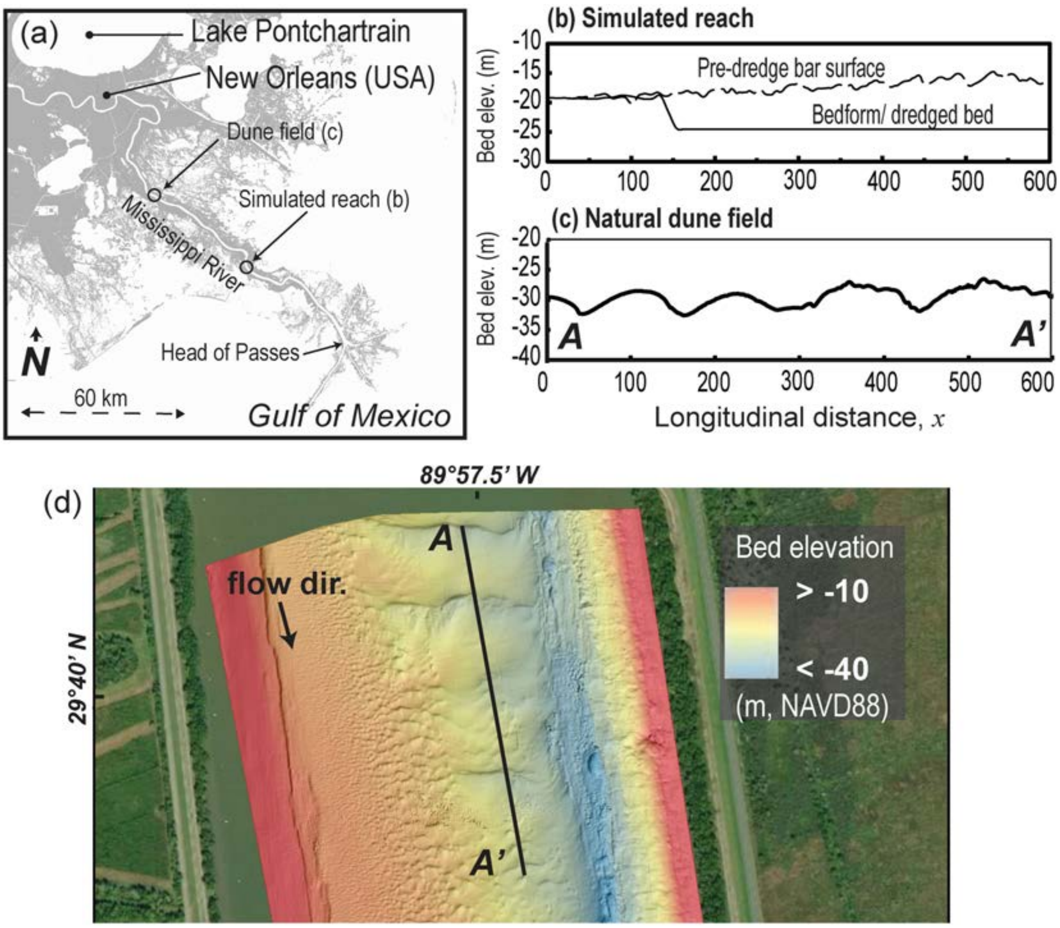

FIGURE 2. (a) The simulated flow in this study is based on that occurring over a channel bar in the lowermost Mississippi River (USA). (b) A longitudinal transect of elevation for the study area before (undisturbed) and immediately after (initial bedform) a dredging campaign that created a large dune-scale bedform. (d) A map of the orientation of this transect. (c, e) Longitudinal and plan view morphology of a nearby natural dune field during a high river discharge (30000 m^3 s^{-1}) for reference. [Colour figure can be viewed at wileyonlinelibrary.com]

and sediment particle velocity are positive net upward, settling velocity is considered positive net downward as per the convention of previous research.

Our study explicitly focused on sediment particle settling as opposed to suspended-sediment transport. Particle settling assumes the termination of movement upon particle contact with the channel bed; particles mobilized by suspended-sediment transport may continue to move upon contact with the bed, dependent on local flow properties. Suspended-sediment transport is generally modelled as the combination of particle settling and particle entrainment (van Rijn, 1984). By focusing on particle settling we can utilize a more physics-based modelling approach than if entrainment processes were also simulated. Entrainment is a complex process reliant on near-bed fluid flow, particle properties, and the composition of the surrounding bed material and it is often modelled using empirical (e.g. Engelund and Fredsøe, 1976; van Rijn, 1984; Garcia and Parker, 1991; McLean, 1992) or stochastic (e.g. Kirchner *et al.*, 1990; Papanicolaou *et al.*, 2002) approaches.

Model development

For our study, we used solvers in the OpenFOAM modeling suite (www.openfoam.org) to simulate sediment-particle movement through a turbulent, 3D open-channel flow field. Our hydrodynamic solver simulated flow dynamics using the non-hydrostatic Navier–Stokes equations for single-phase flow with constant density and viscosity. Turbulence, within the flow field, was simulated using a DES approach (i.e. the Spalart-Allmaras model; Spalart and Allmaras, 1994), which employs a one-equation mixing-length RANS (Reynolds-averaged Navier–Stokes) model to approximate boundary-layer flow near walls and a large-eddy simulation (LES) scheme away from walls. The LES scheme fully resolves turbulent flow dynamics at and above a length scale approximate to the cell dimensions of the computational grid or mesh. Filtering procedures isolate sub-grid spatial scales, where RANS modelling assumptions are also applied to predict turbulent dynamics at that (relatively small) spatial scale. We selected a DES approach for this study because the flow dynamics of interest (eddies large enough to significantly alter medium sand-sized particle settling in the context of a river channel, i.e. length scales on the order of 0.1 to 1.0 m) are located outside of the wall boundary layer in the bedform-wake zone and operate at scales much larger than the anticipated model grid-cell dimensions.

OpenFOAM is a modelling toolbox based on the finite-volume method that has become widely used in the research community because of the open-source code, easy customization, and wide array of available solvers and utilities. OpenFOAM has previously been used to accurately predict open-flow hydrodynamics in natural channels in studies focusing on horizontal recirculation in canyon rivers (Alvarez *et al.*, 2017), river channel evolution by landslides

(Zhao *et al.*, 2017), and flow through vegetation (Chakrabarti *et al.*, 2016), among others (e.g. Badano *et al.*, 2012; Wang, 2013; Lai and Bandrowski, 2014).

We employed the PIMPLE solver in OpenFOAM to calculate pressure and velocity flow-field dynamics. PIMPLE employs either the PISO (pressure implicit with splitting operators) or the SIMPLE (semi-implicit method for pressure-linked equations) algorithm based on stability factors within the model during runtime that allows for adaptive timestep length. Additional numerical methods included an Euler first-order implicit scheme for time discretization, Gaussian linear for discretization of the convective terms, and Gaussian linear corrected for discretization for the Laplacian terms.

We simulated the movement of sediment suspended in flow by one-way coupling of a Lagrangian particle tracking solver (i.e. icoUncoupledKinematicParcelFoam) to the flow solver. The particle-tracking solver calculates the displacement of a prescribed number of mass particles at each time step based on the gravitational and drag forces locally affecting each particle. The particle-tracking solver was modified: (1) to calculate particle response to a time-evolving turbulent flow field and (2) to randomly fluctuate particle-injection locations over a defined depth interval. The coupled solver assigns a unique identification number to each individual particle introduced into the domain and records particle properties including velocities, age, initial injection position, and present position at each output-write interval.

In our modelling analysis, particle-settling velocity (W_P) is defined as the time-averaged vertical particle velocity (U_{ZP}) over a time period of interest (T_0 to T) and timestep t:

$$W_P = \frac{1}{T - T_0}\int_{T_0}^{T} U_{ZP}(t)\partial t \tag{1}$$

The dynamics of the vertical particle velocity is calculated by the particle-tracking solver from the balance of forces pertinent to a spherical object suspended in moving fluid:

$$\frac{\partial U_{ZP}}{\partial t} m_P = F_Z \tag{2}$$

where m_p is particle mass and F_Z is the sum of the most significant forces oriented in the vertical direction, which for a sand-sized particle suspended in the flow column is the particle weight (F_G) plus the vertical drag force (F_{DZ}). Particle mass is calculated as $m_P = \rho_S\, \pi D^3/6$ for a particle with diameter D and density ρ_S. Particle weight is defined as

$$F_G = m_P g\left(1 - \frac{\rho_f}{\rho_S}\right) \tag{3}$$

where g is acceleration due to gravity and p_f is the density of water. The vertical drag force exerted on a spherical particle by fluid flow can be represented by the equations

$$F_{DZ} = C_D \frac{\pi D^2}{8} \rho_f (U_Z - U_{ZP})|U_Z - U_{ZP}| \tag{4}$$

$$C_D = \frac{24}{Re_P}\left(1 + 0.15 Re_P^{0.687}\right) \text{ if } Re_P \leq 1000 \tag{5a}$$

$$C_D = 0.44 \text{ if } Re_P > 1000 \tag{5b}$$

where C_D is the drag coefficient, U_Z is the vertical component of the approach flow velocity, and Re_P is the particle Reynold number given by

$$Re_P = \frac{\rho_f D|U_Z - U_{ZP}|}{\mu} \tag{6}$$

where μ is the dynamic viscosity of water. The particle relaxation time (T_P) is the time it takes the particle velocity to fully respond to a change in the local vertical flow velocity; it is calculated as

$$T_P = \frac{4}{3} \frac{\rho_S D}{\rho_f C_D |U_Z - U_{ZP}|} \tag{7}$$

and is related to the particle drag force as

$$F_{DZ} = m_P \frac{U_Z - U_{ZP}}{T_P} \tag{8}$$

As shown in the equations above, the particle-settling velocity is dependent on the vertical drag force, which itself is dependent on the square of the vertical-velocity differential between the flow and the particle. In turbulent river flow, the vertical flow velocity is comprised of a mean vertical flow velocity ($\overline{U_Z}$) and a fluctuating component (U_Z'):

$$U_Z = \overline{U_Z} + U_Z' \tag{9}$$

Over distances and timescales applicable to the settling of a sediment particle in large flat-bedded rivers, $\overline{U_Z} \approx 0$, so for practical purposes the vertical drag force becomes dependent on the differential between the fluctuation of the vertical flow velocity and the vertical particle velocity. In turbulence research, a common metric used to characterize the intensity of the velocity fluctuations is calculated as the root-mean-square value for a time series of fluctuation values. In our study, the root-mean-square of the vertical-velocity fluctuations ($U_Z'_{RMS}$) is of importance and is defined as:

$$U_Z'_{RMS} = \sqrt{\frac{1}{T - T_0}\int_{T_0}^{T} \left[U_Z'(t)\right]^2 \partial t} \tag{10}$$

Turbulence becomes effective at suspending particles in the flow column when $U_Z'_{RMS}$ values approximate or exceed the particle still-water settling velocity (Middleton and Southard, 1984; Raudkivi, 1998). In rivers, undulations in the channel bed, such as bedforms, create currents with persistent nonzero vertical velocities through topographic steering; in these currents, as well as in channels with significant secondary flows, particle settling will be dependent on both $\overline{U_Z}$ and U_Z' locally.

The particle-tracking solver assumed that the particle settling was dependent on the drag force exerted by the flow and the particle weight. Other forces, such as lift, were not incorporated into the modelled physics because (1) they were calculated to be an order of magnitude or less than the drag force and weight for suspended particles in our model or (2) their influential physics were not practically resolvable at our model scale. Previous studies using Lagrangian particle tracking to simulate sediment transport in rivers relied on the same simplifying assumption (e.g. Shams *et al.*, 2002; Pasiok and Stilger-Szydło, 2010; Allison *et al.*, 2017).

Model setup

The model was set up to simulate flow and sediment transport in realistic flow conditions typical of the lower Mississippi River using the study site shown in Figure 2 as a template. The model domain was 600 m long and 20 m wide. Flow depth through the domain was variable, ranging from approximately 19 to 25 m, and based on the channel bathymetry of the simulated study site. While we focused our analyses in this study on flow and sediment transport in the downstream (*x*) and vertical (*z*) dimensions, we found that it was necessary to simulate horizontal flow (i.e. in the *y* dimension) to properly resolve turbulent eddy development and dissipation using the DES approach. We developed two different meshes for the model domain (Figure 3). Mesh cell size was approximately 0.33(*x*) × 0.5(*y*) × 0.33(*z*) m. Each mesh had a sub-area of cell refinement (the resolution was increased by a factor of two) designed to better resolve the flow field around the simulated bedform. The bedform was oriented so that the lee-side slope began 100 m downstream of the domain inlet. We included a zone of refinement in the mesh with a flat bed (mesh B in Figure 3) for consistency. The total number of mesh cells was 8.4 (mesh A) and 5.5 million (mesh B).

We sized the mesh cells to resolve a predominant fraction (>80%) of the turbulent kinetic energy generated from the bedform wake. We tested this criterion by calculating the probability distribution of the most active turbulent length scales using the integral length scale (size of the largest, most-energetic eddies) and Kolmogorov length scale (smallest effective eddy size) as reference. These turbulence scales were computed from the distributions of turbulent energy production and dissipation values predicted from an auxiliary K-epsilon RANS model of the same domain (as per the theory discussed in Umlauf and Burchard, 2003; Wang *et al*., 2015).

Velocity boundary conditions were set as zero gradient at the downstream boundary, 'no-slip' at the bottom boundary, and 'slip' at the surface and lateral boundaries. The inlet boundary was set as 'mapped', which recycled flow patterns derived from an internal location (near the outlet) to simulate a well-developed turbulent profile with a prescribed depth-averaged velocity and has been used in similar studies (e.g. Schmeeckle, 2014).

The particle-tracking model injected mass particles down a central vertical profile (extending from the water surface to a depth of −18 m) immediately upstream of the location of the bedform crest in Figure 3a (i.e. at $x = 100$). Particle injections were uniformly distributed along the vertical profile at a prescribed rate. While sand-sized particles are typically transported vertically stratified in river flow, we chose the uniformly distributed sediment feed to simplify interpretation of the simulation results. In the case of a uniform vertical particle feed, differences in the longitudinal pattern of sediment would be predominantly a result of the properties of the flow field.

For each simulation, the model was run for 6000 s to initialize a steady-state flow field through the full model domain before the particle feed began. The total duration for the simulation of each scenario (Table 1) was set to exceed the length of time required to establish a steady-state particle deposition pattern. A steady state was assumed to be obtained when the deposition pattern became insensitive to additional simulation time as analysed at 1000 s intervals. For this analysis, once particles touched the bottom boundary (i.e. the channel bed), they became immobile and were recorded as deposited. Deposition in our model is a simplification of sediment deposition processes that occur in natural rivers where, upon contact with the channel bed, sediment particles can continue to move as bedload or become resuspended in the flow column.

The model was run on the Cypress high-performance computing (HPC) cluster at Tulane University (New Orleans, USA). Each model run was parallelized on 160 processors. Typical model run times were on the order of 5–7 days. The maximum Courant number was restricted to 0.5; typical model time steps ranged from 0.001 to 0.05 s for simulations employing the DES turbulence model.

Further description of model parameterization, including discretization schemes, solvers, and wall function properties, is included in the online Supporting Information.

Model scenarios

For the 3D modelling analysis, we simulated four scenarios. The text below includes a brief description of each scenario. Table 1 summarizes the key scenario properties.

Scenario 1: the reference scenario

The objective of this scenario was to investigate sediment-particle settling over a large, simple bedform with resolved turbulence. The scenario bathymetry was set to approximate the channel bathymetry for the site shown in Figure 2b after it was modified by dredging. This bathymetry (mesh a in Figure 3) simulated a large, simplified dune-scale bedform. The lee-side slope of the bedform, located between $x = 100$ and $x = 150$, composed the primary morphological feature within the

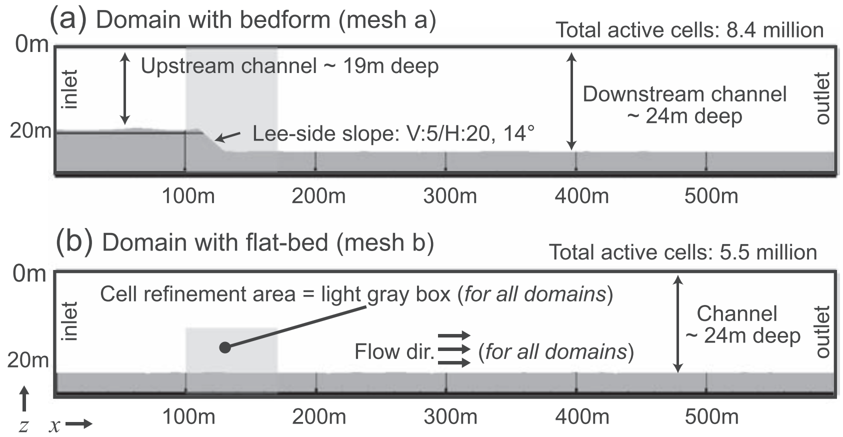

FIGURE 3. Schematic of the two different model domain variations, mesh a and b. Each box shows a profile view of a domain variation; the white area is the area open to flow, the dark-grey area at the box floor represents ground and is closed to flow.

Table 1. Summary of key scenario properties

Scenario	Bed morphology[a]	Impact of bedform on flow	Resolved turbulence[b]	Bedform-generated turbulence	Background turbulence
1. Reference	bedform	yes	yes	yes	yes
2. Static velocity	bedform	yes	no	no	no
3. Flat bed	flat	no	yes	no	yes
4. Flat bed, static velocity	flat	no	no	no	no

[a]bedform = mesh a; flat = mesh b.
[b]yes = employed detach eddy simulation; no = static velocity field.

domain. The mean flow velocity (1.5 m s^{-1}) through the domain inlet was set to approximate the depth-averaged velocity of a moderate discharge for the lower Mississippi River.

Scenario 2: the static-velocity field scenario
This scenario employed a static (or 'frozen') velocity field equal to the temporally averaged flow field of Scenario 1. This scenario simulated sediment particles settling through the same mean velocity field as Scenario 1, with no temporal variability in flow velocity. The simulation of this scenario served as a method to investigate particle settling in the absence of turbulent fluctuations in the flow field.

Scenario 3: the flat-bed scenario
The objective of this scenario was to investigate sediment-particle settling absent of a bedform on the flow field. In this scenario, only 'background turbulence' (i.e. that introduced through the inlet or generated from the channel bed) was resolved. For this scenario, the relatively deep channel bed downstream of the bedform from Scenario 1 was extended upstream to fill the full domain (mesh b; see Figure 3b). The mean velocity at the inlet was set to the same value as the mean velocity in the channel downstream of the bedform from Scenario 1 (i.e. 1.18 m s^{-1}). Unlike the other scenarios that introduced velocity fluctuations at the inlet by mapping the velocity field to that of a downstream location with a well-developed turbulent velocity profile, in this scenario the inlet flow velocity was prescribed as a uniform value with a randomized fluctuation component. The fluctuating component of the inlet velocity was designed to replicate the same approximate turbulent intensity in the upstream channel as Scenario 1 (measured at x = 50). This method was used to ensure that the mean 'background turbulence' intensity of the flow entering the model domain was approximate to that in Scenario 1.

Scenario 4: the flat-bed, static-velocity scenario
This scenario was the same as Scenario 3 except that it used a static velocity field equal to the temporally averaged flow field from Scenario 3. The objective of this scenario was to investigate sediment-particle settling in the absence of (1) turbulent fluctuations and (2) the impact of the bedform on the flow field.

Model validation

Our objective for the 3D model analyses was to simulate particle settling through realistic turbulent flow fields generally and not to precisely replicate site-specific flow hydrodynamics. Therefore, formal calibration and validation testing against observed hydrodynamic measurements lies outside the study scope. We did perform two series of sensitivity tests to investigate how well the Spalart-Allmaras DES turbulence model simulated realistic bedform-generated wake properties in river-like flow conditions. The objective of the first series of tests was to examine how well a 3D OpenFOAM CFD model, parameterized the same as that used developed in this study, replicated the results of a robust flume study of dune-generated turbulence (Kwoll *et al.*, 2016). The tests compared model predictions of flow velocity and turbulence with values observed in the laboratory over 30, 20, and 10° lee-side angle dunes. The objective of the second series of tests was to re-size the model used in the first series of tests, which had computational mesh cell dimensions on the order of 10^{-3} m, to a larger scale suitable for simulating hydrodynamics at a real-world river scale, i.e. with mesh cell dimensions on the order of 10^{-1} m (the same dimensions employed by the main model used in this study). The second series of tests was necessary because the simulation of turbulence is sensitive to mesh cell size; we wanted to ensure that an upscaled model which performed well in simulating hydrodynamics and turbulence at the flume scale would not perform substantially differently at the field scale.

The results of these tests indicated that the largest discrepancies between the modelled and observed hydrodynamic values were related to (1) velocity gradients very near the bed and (2) the extent of the turbulent wake. The modelled near-bed streamwise and vertical velocities had errors ranging from 5 to 20% at the mesh cell scale, with the highest errors located at the bedform-wake margins. The model tended to overestimate the area of intense turbulence in the bedform wake (from 10 to 50%) and slightly underestimate turbulent intensity at the transition between the wake and the ambient flow column, which decreased the apparent extent of the modelled wake relative to that observed (by up to ~25%). The results of our mesh scaling validation exercise indicated that the range of cell sizes tested did not significantly influence the flow velocity and turbulence fields.

Interpretation of our validation results suggests that our parameterization of the hydrodynamic and turbulence model simulated flow-velocity magnitude and fluctuations in the range that occurs in real-world rivers. The primary difference between the modelled and observed flow field was that the model predicted more intense and spatially concentrated turbulence within the bedform wake. This discrepancy was likely due to the simplicity of the model domain, which could not fully replicate the variability in the flume flow. Unlike the modelled flow, the flume flow was impacted by velocity shear at the flume walls and the free surface, and by turbulence generated from mechanical flow recirculation. The impact of these phenomena would add more turbulence generally through the flow column and diffuse turbulence specifically generated in the bedform wake. The elongated flume channel would likely generate secondary currents absent in the (shorter) validation model, which would add further discrepancies in complexity between the flume and the model flow.

Flow in natural channels would be far more complex than that simulated in the flume or in our model domains due to the presence of asymmetries in the natural channel morphology, irregular planform (e.g. channel meandering), and obstacles to flow (e.g. large sediment grains, vegetation, debris). The complex flow patterns in natural channels would likely have the net effect of further diffusing the intensity of the bedform-generated turbulence throughout the wider flow column. Therefore, our estimation of the influence of bedform-generated turbulence on particle settling in this study, which does not include this flow complexity, would likely be near the maximum strength expected in nature.

Results of the validation tests are further detailed in the online Supporting Information.

Results

Simulation of the flow field

Simulated flow over a bedform

Our model appeared to simulate realistic flow patterns and turbulence fields well; the turbulent intensities and scales of the modelled flow were on the same relative magnitude as those measured in observed river channels with similar geomorphic properties (McQuivey, 1973). In our 'reference' scenario, which simulated turbulent flow and particle transport over a large bedform (Figure 4), the model predicted a range of persistent flow characteristics. Depth-averaged flow velocity was reduced by 21% in the deeper channel downstream of the bedform (referred to as 'the downstream channel' herein) relative to the channel upstream of the bedform (referred to as 'the upstream channel' herein). Reach-averaged boundary shear stress was reduced by 30% on the downstream channel bed relative to the upstream channel bed. Flow through the upstream channel maintained a relatively uniform velocity profile. The drop in bed elevation through the lee-side slope of the bedform influenced the flow similar to a naturally formed subaqueous dune (such as that documented in Parsons *et al.*, 2005).

In the reference scenario, a significant zone of flow separation with occasional flow recirculation developed on the lee side of the bedform. This zone was typically on the order of 20 m long and intermittently extended an additional 10–20 m. The largest turbulent intensities corresponded to the downstream margins of the flow separation zone ($x = 140$–160; see Figure 5), which was the location of the greatest velocity shear. Large turbulent eddies developed downstream of the bedform and were advected with the downstream current. These eddies typically persisted during their transport through the model domain, growing in size and becoming more amorphous with distance downstream. The eddies tended to display an advection (lift-off) angle of between 5 and 15°.

Figure 4b shows an example of the vertical-velocity field associated with eddies in the bedform wake. The large eddies, with characteristic dimensions ranging on the order of 10^0 to 10^1 m, produced frequent and relatively steep vertical velocity gradients.

The 'static-velocity' scenario produced a relatively simple spatial distribution of flow velocities (Figure 6a). Flow velocities increase monotonically with distance away from the lee side of the bedform and the channel bed through the bottom half of the model domain. The steepest gradient in flow velocities occurred downstream of the bedform crest, where flow velocities transitioned from the order of 0.1 to 1.5 m s^{-1} in a distance on the order of 5 m.

Simulated flow over a flat bed

Figures 6b and c show example instantaneous flow fields for the 'flat-bed' and the 'flat-bed, static-velocity' scenarios,

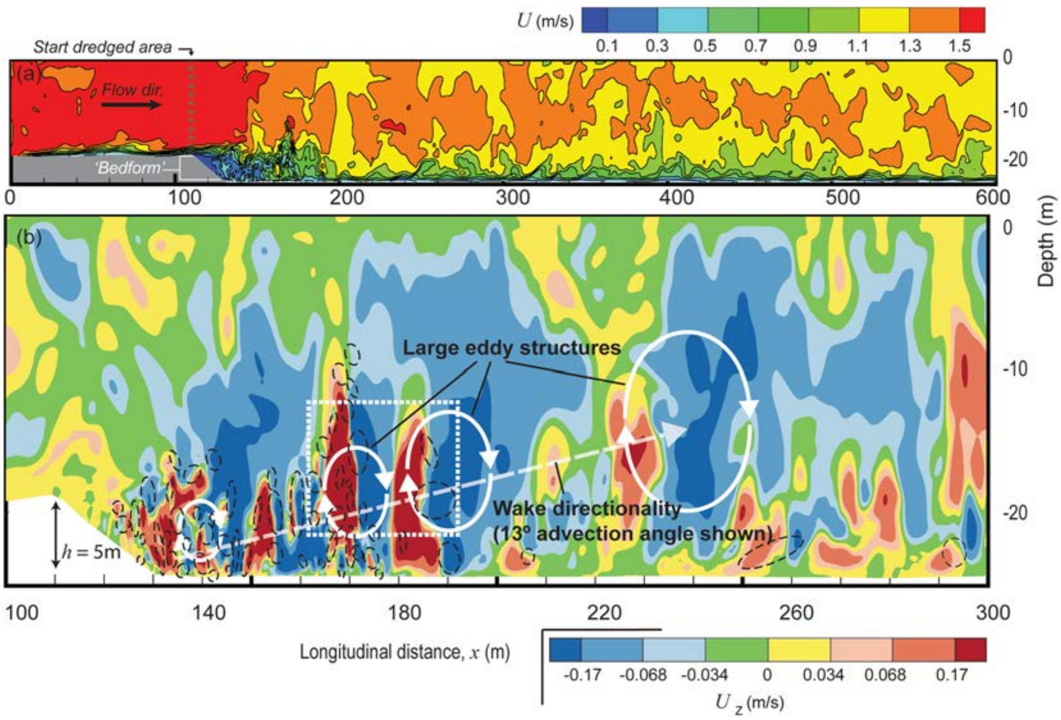

FIGURE 4. (a) An example of the modelled instantaneous flow-velocity field extracted down the model domain centre line for the 'reference' scenario. (b) The vertical component of a subsection of the velocity field immediately downstream of the bedform; examples of resolved large eddy structures and the mean directionality of the bedform wake are annotated. The dashed black ovals outline the centre of vortex-like features [i.e. where the Q-criterion, a metric of the balance between fluid rotation and strain (Dubief and Delcayre, 2000) – is >0.1]. The white dashed box in (b) shows the approximate location of the data illustrated in Figure 6. [Colour figure can be viewed at wileyonlinelibrary.com]

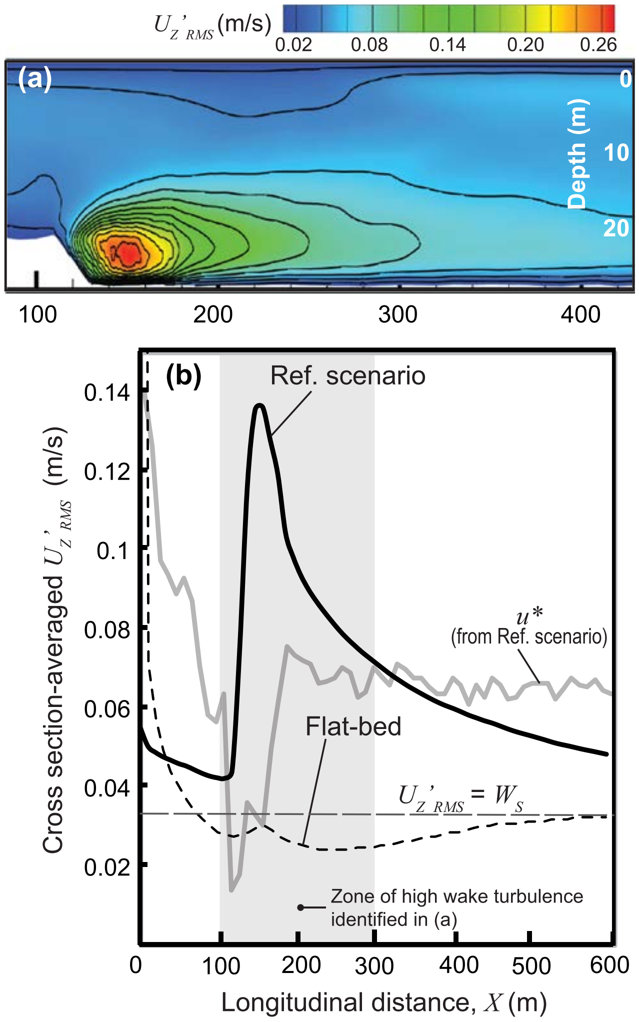

FIGURE 5. (a) Temporally averaged vertical turbulence intensity (in terms of $U_Z{}'_{RMS}$) down the longitudinal centre line of the model domain for the 'reference' scenario. (b) Cross-section-averaged vertical-turbulence intensity by longitudinal distance for model scenarios that resolve flow turbulence. Generally, $U_Z{}'_{RMS} > Ws$ is considered a criterion to maintain sediment suspension through diffusive mixing in alluvial channels (Raudkivi, 1998); this criterion is delineated on the plot for reference. The grey box shows the zone of high wake turbulence as interpreted from (a). Time-averaged shear velocity ($u*$) calculated from the 'reference' scenario flow field is also shown for reference. [Colour figure can be viewed at wileyonlinelibrary.com]

respectively. As stated previously, the 'flat-bed' scenario employed a prescribed input of uniformly distributed, random turbulence at the inlet. The level of prescribed turbulence was set to replicate the same mean intensity as that calculated in the channel upstream of the bedform in the 'reference' scenario. Because the 'flat-bed' scenario did not employ a 'mapped' velocity boundary condition at the inlet, a turbulent vertical-velocity profile did not fully develop until $x > 100$ m. The flow field of the 'flat-bed, static-velocity' scenario displayed a logarithmic vertical-velocity profile that is typical of flow through rough-bedded open channels and was approximately uniform in the horizontal dimensions.

Predicted distributions of the vertical-velocity fluctuations

Figure 7 displays the joint distributions for the streamwise and vertical-velocity fluctuations for the 'reference' scenario calculated at three points distributed longitudinally, i.e. $x = 150$, 300, and 550. The values in the figure were all calculated at a central cross-stream location ($y = 10$ m) and in the vertical plane with the highest mean turbulence values ($z = -20$ m, i.e. the approximate bedform crest elevation). Turbulence data in each plot were sampled from the flow field at 20 Hz for 2000 s. This frequency and sampling period allowed for multiple velocity samples of a sufficient number of eddies (such as that defined in Luchik and Tiederman, 1987) to establish summary statistics that were insensitive to the addition of further data. The plots are indicative of quadrant analysis used in environmental turbulence studies that separate turbulent events into four types of turbulent event: (i) outward interactions, (ii) ejections, (iii) inward interactions, and (iv) sweeps (numerals correspond to those used in Figure 7). Typically, quadrant analysis is used to characterize turbulence generated from shear within the near-bed flow; however, here we use it to illustrate the magnitude and frequency of vertical-velocity fluctuations and their general relationship with downstream-flow fluctuations within the zone of highest turbulence intensity. In river flow, vertical-velocity fluctuations are typically considered a first-order control of suspended-sediment behaviour (Raudkivi, 1998).

In Figures 7a–c, the mean velocity fluctuation magnitudes and standard deviations decline with distance from the bedform (Table 2). The distribution of velocity fluctuations shown in Figure 7c was similar to the distribution of velocity fluctuations for the flat-bed scenario at the same location (Figure 7d), suggesting that the influence of the bedform-generated turbulence had degenerated to a similar intensity as that produced by modelled background turbulence. For the 'reference' scenario, ejection and sweep events were by far the most frequent types of turbulent fluctuation event. While both ejection and sweep events have been shown to positively contribute to the suspension of bed material through the positive generation of turbulence and Reynolds stresses (Bennett and Best, 1995; Nelson *et al.*, 1995; Cellino and Lemmin, 2004; Kwoll *et al.*, 2016), from a general perspective, ejection events would reduce particle-settling velocities and sweep events would increase particle-settling velocities due to their relative vertical orientations. While sweep events were somewhat more frequent than ejection events, the mean magnitudes of ejection events were greater than the mean magnitudes of sweep events.

Simulation of the suspended particles

Modelled suspended-particle fields

The simulated vertical-velocity fields appeared to have a substantial influence on the suspended-particle fields, in terms of the instantaneous vertical particle velocities (U_{ZP}) and particle trajectories (Figure 8). Analysis of the model results indicates that, for the vast majority of the simulation, U_{ZP} was equal to U_Z plus W_S (Figure 9). Differences between particle and local-flow vertical velocities were typically greatest in the most turbulent areas of flow and were attributed to the response time it took the flow current to accelerate a particle to the current velocity upon initial contact. The particle relaxation time (T_P) calculated by Equation (7) predicts that, for medium sand in the flow conditions simulated, particles reached local current velocities approximately 0.01–0.05 s after initial contact with the current.

The four different scenarios simulated by the model produced substantial variations in the predicted suspended-particle fields in terms of the number of particles in suspension (relative to the particle feed at the model inlet) and in spatial distribution. Figure 10 shows the simulated suspended-particle fields at the conclusion of the model run for the four scenarios. The spatial distribution of the particles in the scenarios that resolved turbulence appears more chaotic relative to the scenarios with static-velocity fields due to mixing

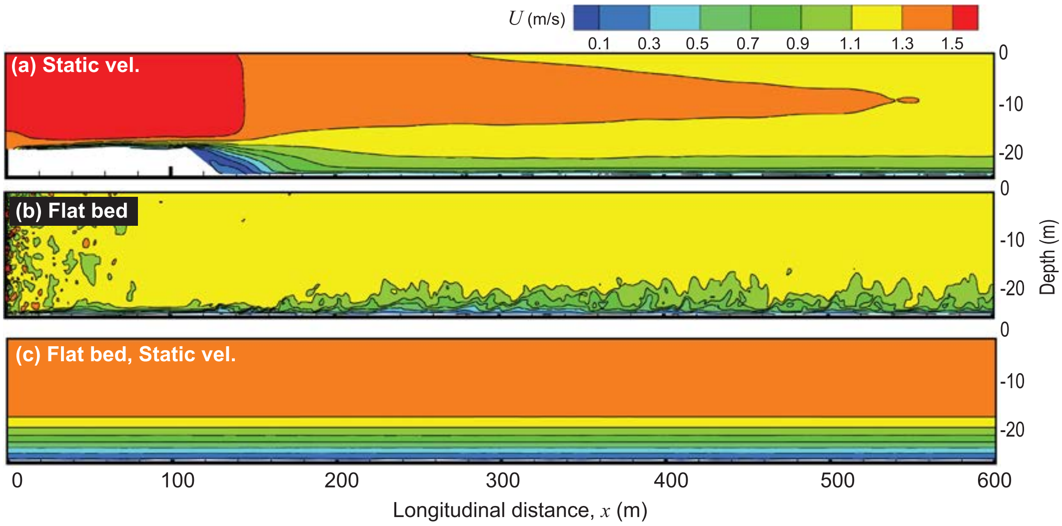

FIGURE 6. Examples of the predicted instantaneous velocity fields extracted down the centre line of the model domain for (a) 'static-velocity', (b) 'flat-bed', and (c) 'static-velocity, flat-bed' scenarios. [Colour figure can be viewed at wileyonlinelibrary.com]

within and around the turbulent eddies. The eddy-induced mixing created spatial clusters of particles with similar vertical velocities. These particle clusters diffused with distance downstream. The cluster sizes observed in the 'flat-bed' scenario were generally smaller than those in the 'reference' scenario. Eddies in the 'flat-bed' scenario were solely a product of velocity shear at the bed, as opposed to the 'reference' scenario which included eddies generated from bedform wake.

The particle mixing occurring in the turbulence-resolving scenarios maintained much more vertically uniform particle concentration profiles throughout the length of the model domain than that calculated in the scenarios without

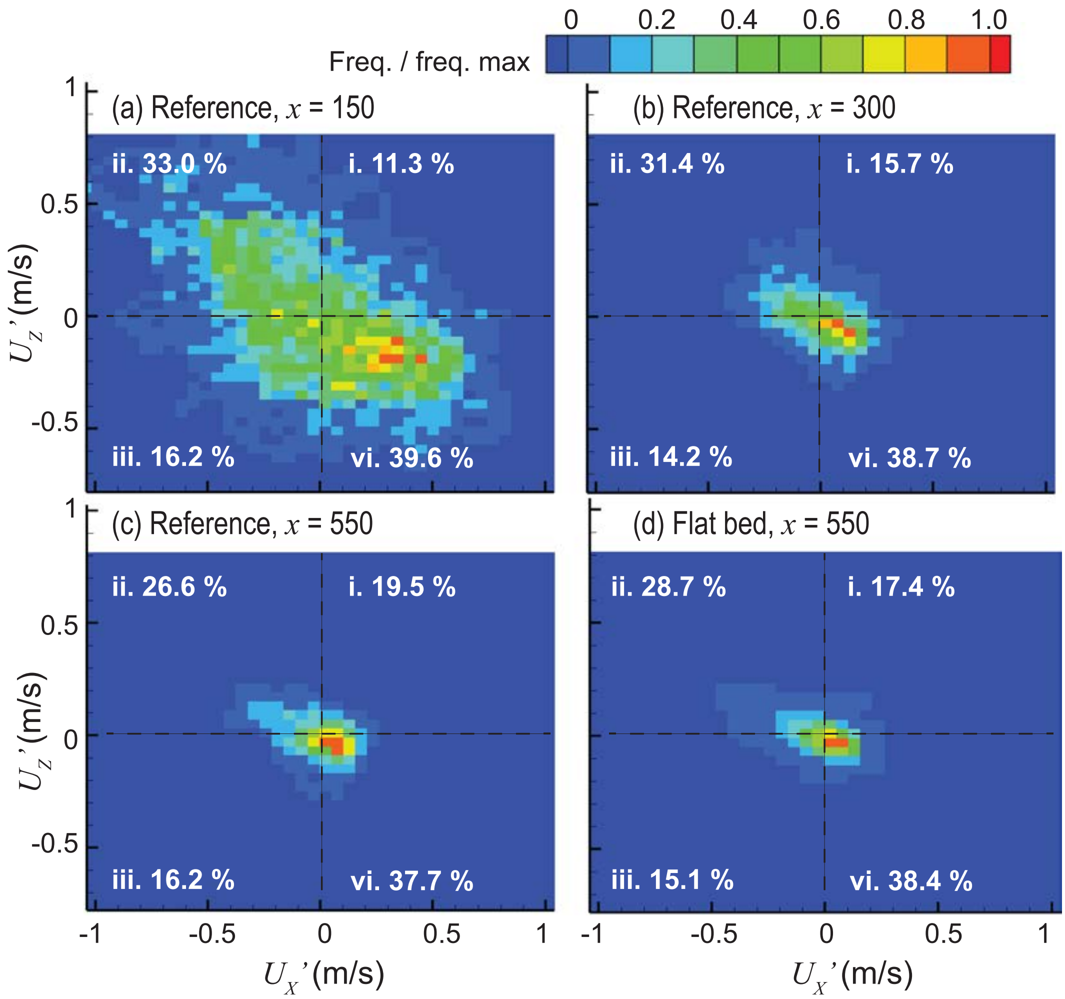

FIGURE 7. Joint frequency distributions for streamwise (U_X') and vertical (U_Z') velocity flucuations illustrated in quadrant analysis plots. Values in the quadrant corners show the percentage of the total data points present in that quadrant. (a, b, c) Data for the 'reference' scenario calculated at locations $x = 150$, 300, 550, respectively. (d) Data for the 'flat-bed' scenario at $x = 550$. [Colour figure can be viewed at wileyonlinelibrary.com]

Table 2. Summary statistic of the vertical velocity fluctuations shown in Figure 7 by quadrant

Scenario/location	Statistic	Quadrant (i) U_Z' (ms^{-1})	(ii) U_Z' (ms^{-1})	(iii) U_Z' (ms^{-1})	(iv) U_Z' (ms^{-1})
	mean	0.147	0.283	−0.169	−0.209
Ref./$x = 150$	Std. dev.	0.133	0.183	0.122	0.128
	mean	0.062	0.091	−0.057	−0.078
Ref./$x = 300$	Std. dev.	0.056	0.069	0.048	0.056
	mean	0.038	0.079	−0.045	−0.056
Ref./$x = 550$	Std. dev.	0.029	0.053	0.035	0.042
	mean	0.033	0.059	−0.036	−0.044
Flat-bed/$x = 550$	Std. dev.	0.030	0.043	0.030	0.032

turbulence (Figure 11a). This particle mixing is likely responsible for maintaining the significantly higher depth-averaged particle concentrations calculated for the 'reference' scenario relative to the 'static-velocity' scenario downstream of $x = 500$ (Figure 11b).

Predicted particle-settling velocities

Figure 12 shows the relative impact of bedform-generated turbulence and background turbulence on the particle-settling velocities. While bedform-generated turbulence is primarily directional, background turbulence may have both significant directional (upwelling from the near-bed velocity shear) and isotropic properties (Murray, 1970). Figure 12a shows particle settling in bedform-generated turbulence and illustrates that, in the zone of intense wake turbulence ($x = 100$–300), particles were entrained in eddies developing in the velocity shear zone on the lee side of the bedform and were lifted upward through the flow column. Further downstream, the turbulence generated from the dissipating eddies kept the particles well mixed throughout the depth profile and maintained the suspension of the previously lifted particles within the upper flow column (as suggested by the prevalence of particles with net upward trajectories, i.e. $W_P/W_S < 0$) in the figure.

Figure 12b shows that the particles settling through background-only turbulence (i.e. 'the flat-bed' scenario) were slightly more mixed through the flow column than in the absence of turbulence (i.e. the 'flat-bed, static-velocity' scenario), but were less mixed than when impacted by bedform-generated turbulence. Clusters of particles with similar settling velocities formed and remained relatively coherent through background-only turbulence; these clusters were less common in the 'reference' scenario, likely due to the more intense mixing caused by the bedform-wake turbulence.

Figure 13 illustrates the summary statics calculated for the particle-settling velocities shown in Figure 12. Figure 13a shows that the range of particle-settling velocities was much wider in the presence of bedform-generated turbulence (i.e. the 'reference' scenario) than in background-only turbulence (i.e. the 'flat-bed' scenario). For both scenarios, the distributions of particle-settling velocities stabilized through the downstream half of their domain and appeared to begin to converge to a similar, relatively small range of values. The median

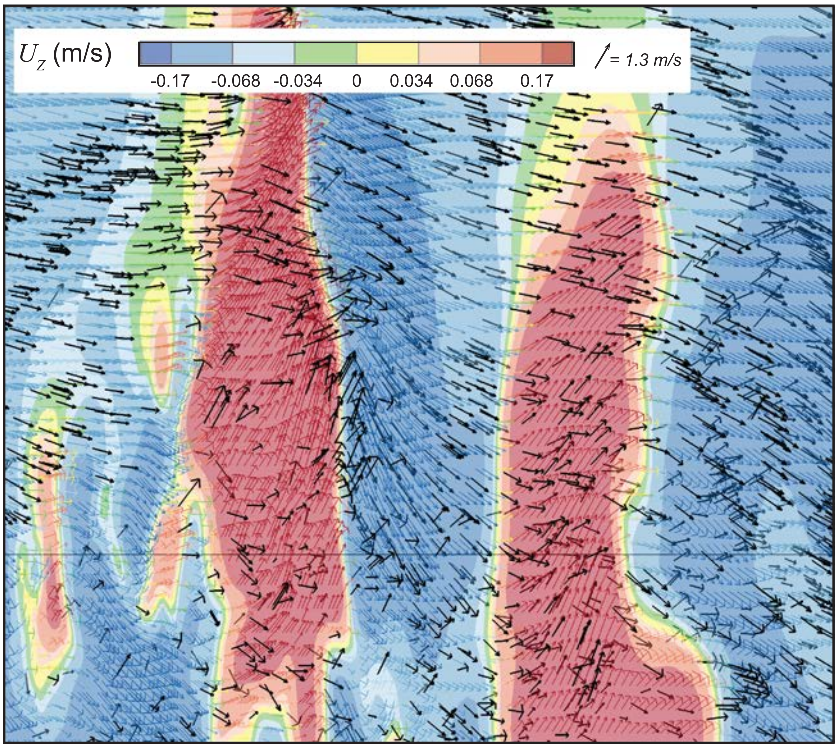

FIGURE 8. A zoomed-in view of the vertical-velocity field shown in Figure 4b. The coloured arrows are flow velocity vectors for the velocity field; the black arrows show the velocity vectors for sediment particles suspended within the flow field (i.e. extracted along the same central longitudinal transect). [Colour figure can be viewed at wileyonlinelibrary.com]

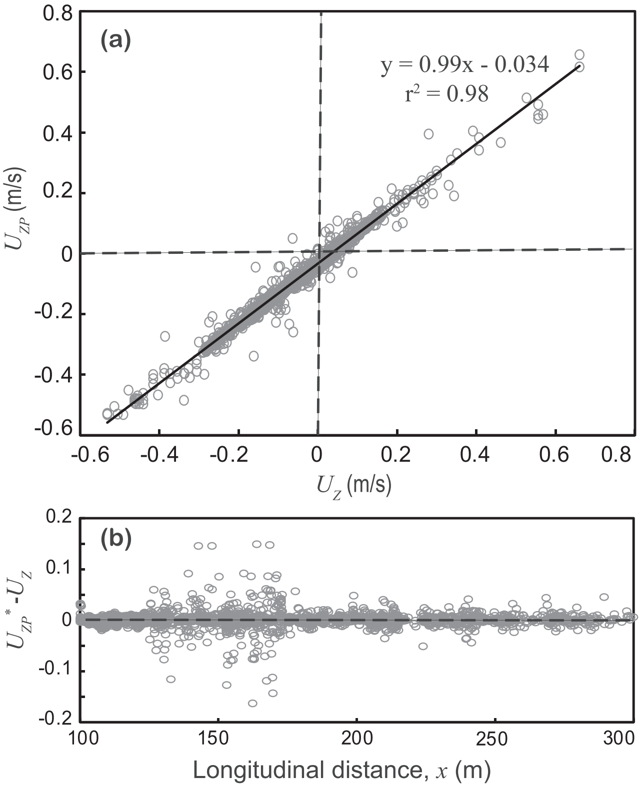

FIGURE 9. Plots of the relationship between instantaneous vertical-particle velocity (U_{ZP}) and the surrounding vertical-flow velocity (U_Z) field for suspended particles between x = 100 and x = 200 at the conclusion of the 'reference' scenario simulation: (a) the relationship between U_Z and U_{ZP}; (b) the difference between U_Z and U_{ZP}* (U_{ZP}* is the vertical-particle velocity with the impact of the particle still-water settling velocity negated; i.e. $U_{ZP}^* = U_{ZP} + W_S$) by longitudinal position.

settling velocity of the 'reference' scenario was substantially reduced relative to the median settling velocity of the 'static-velocity' scenario through the wake zone and became reduced relative to the still-water settling velocity near the downstream end of the domain. The median settling velocity for the 'flat-bed' scenario was generally less than the

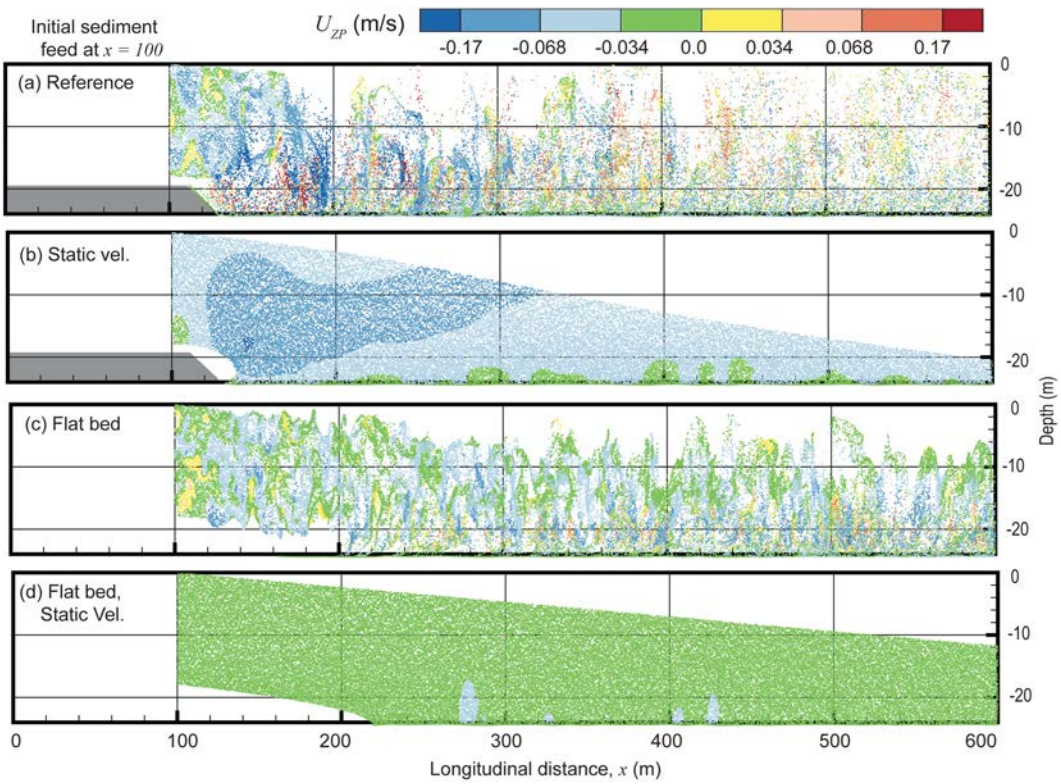

FIGURE 10. Examples of the predicted instantaneous particle concentration fields for (a) 'reference', (b) 'static-velocity', (c) 'flat-bed', and (d) 'static-velocity, flat-bed' scenarios. Individual sediment particles are coloured by their vertical velocities; note that negative vertical velocities are upwards. The number of visible particles was reduced by a factor of 2 to promote clarity. [Colour figure can be viewed at wileyonlinelibrary.com]

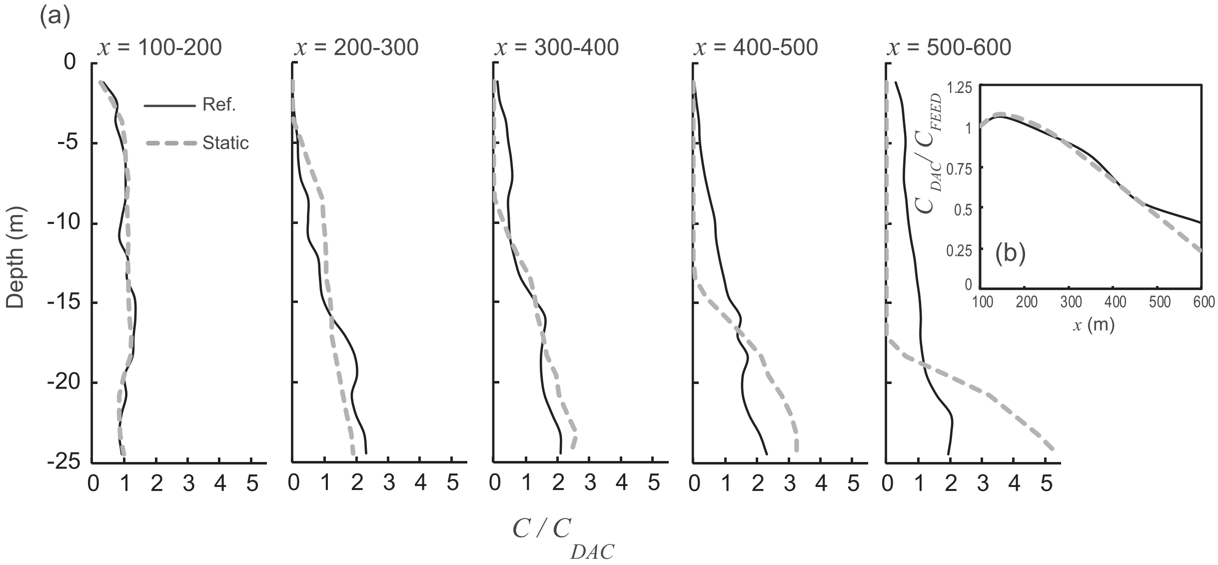

FIGURE 11. Instantaneous particle concentrations for the 'reference' and 'static-velocity' scenarios. (a) Spatially averaged vertical concentration profile binned at 100 m intervals; concentration values (C) are standardized by the depth-averaged concentration (C_{DAC}) at each location. (b) Approximate depth-averaged particle concentrations for the same scenarios by longitudinal distance; in this plot, the particle concentration values are standardized by the concentration of the initial feed at the inlet (C_{FEED}).

still-water settling velocity through the majority of the model domain.

The differences in median particle-settling velocity for the 'reference' and the 'flat-bed' scenarios relative to their counterpart scenarios that did not simulate turbulence (i.e. the 'static-velocity' and the 'flat-bed, static-velocity' scenarios, respectively) were calculated and are shown in Figure 13b. The magnitude of the difference values increased with longitudinal distance, which suggests that particle suspension became increasingly dependent on the interaction of the particles with the resolved turbulence as the particles travelled downstream. Approaching the domain outlet, turbulence resolved in the 'flat-bed' scenario (i.e. that resolving 'background' turbulence) decreased the median settling rate for suspended particles by approximately 0.01 $m s^{-1}$ (an ~30% reduction). The turbulence resolved in the 'reference' scenario (i.e. that resolving 'background' and 'bedform-generated' turbulence) decreased the median settling rate by approximately 0.025 $m s^{-1}$ near the domain outlet (an ~50% reduction). The reduction of particle-settling velocities due to turbulence had a significant impact on the percentage of suspended particles that were deposited on the domain bed during the associated simulations (Table 3).

Discussion

Influence of bedform-generated turbulence on particle settling

Our modelling analyses indicate that the bedform-generated wake substantially reduced the settling velocities of particles passing through it. From our analyses, we cannot precisely identify the underlying mechanics of this settling reduction; however, we can infer some of the influential processes contributing to the reduced particle settling from the modelled flow and particle fields. As we show, the vertical particle velocity was closely correlated to the vertical flow velocity. The bedform-generated turbulence does not increase mean upward oriented velocities relative to scenarios without bedform-generated turbulence; however, it may modulate

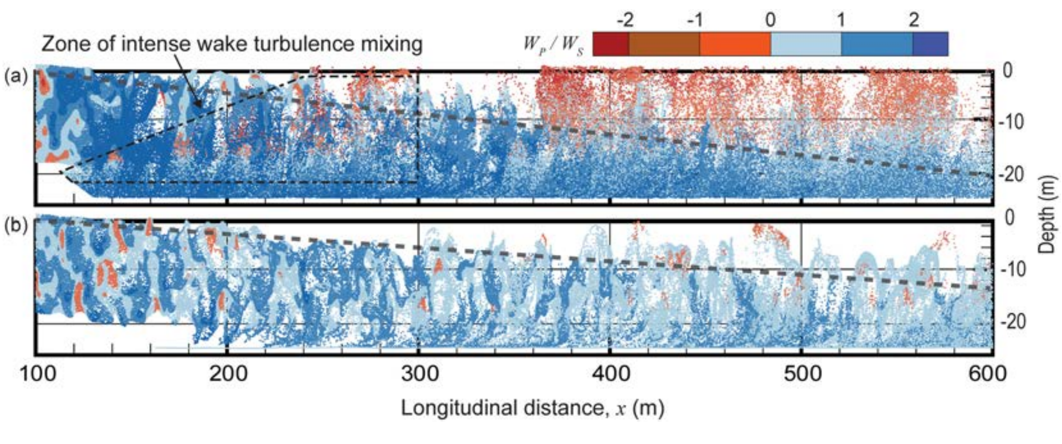

FIGURE 12. Plots of the instantaneous field of particles suspended in flow, coloured by relative settling velocity (W_P/W_S) for (a) 'reference' and (b) 'flat-bed' scenarios. The thick-dashed line delineates the upper bounds of the particle distributions for the (a) 'static-velocity' scenario and (b) 'flat-bed, static-velocity' scenario for reference. The approximate zone of the most intense particle mixing and upwelling due to wake turbulence is shown as a dashed black polygon in (a). The plots illustrate the same particle fields as shown in Figures 10a and c without reducing the number of visible particles. [Colour figure can be viewed at wileyonlinelibrary.com]

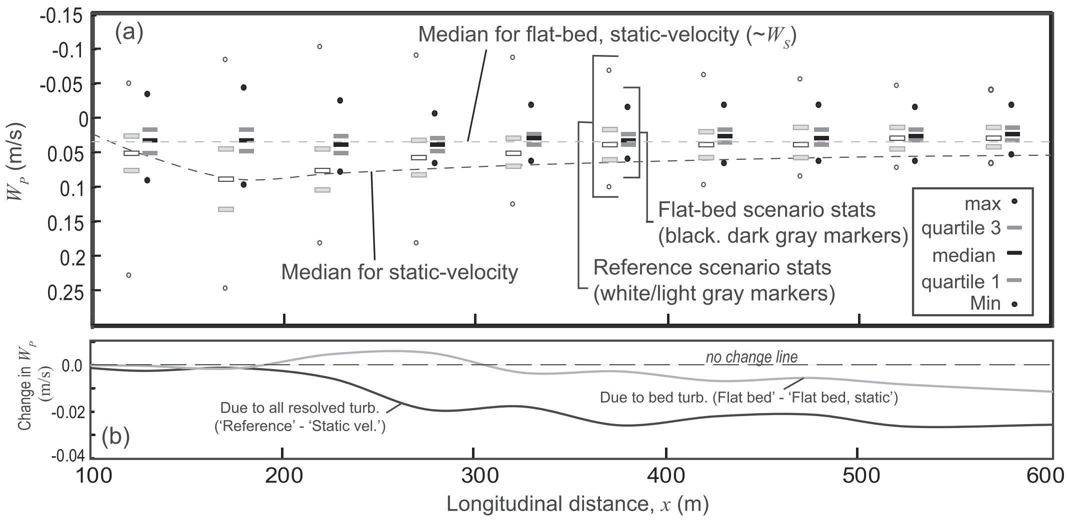

FIGURE 13. (a) Summary statistics, in box-and-whisker format, of the distributions of particle-settling velocities shown in Figure 12, binned at 50m spatial intervals in the *x* direction. The median particle-settling velocities estimated for the static-velocity scenarios are shown for reference; the median particle-settling velocity for the 'flat-bed, static velocity' scenario is approximate to the still-water settling velocity (W_S). (b) Change in median particle-settling velocity, as shown in (a), for the scenarios where turbulence is resolved relative to the static-velocity scenarios.

velocity fluctuations in a way that enhances the influence of the upward fluctuations relative to the downward fluctuations on vertical particle velocities.

Similar to observations reported in many studies of bedforms (e.g. Lapointe, 1992; Kostaschuk, 2000), our study shows that the bedform wake is primarily composed of eddy structures that are generated in the velocity shear immediately downstream of the bedform and that translate downstream and upwards, away from the bed. While these eddies do not produce a net upwards flow throughout the wake area, our modelling indicates that they do impact the vertical flow in significant ways. Figure 7 and Table 2 indicate that while downward velocity fluctuations are typically more frequent than upward velocity fluctuations, upward fluctuations are, on average, higher in magnitude. These observations appear to be aligned with the typical eddy structures qualitatively identified in Figure 4. In Figure 4, the fraction of the eddy with net downward flow is relatively large and slow moving, while the fraction composed of new upward flow was smaller and swifter, on average. We hypothesize that this asymmetry in the balance of the magnitude and frequency of upward and downward velocity fluctuations may act as a potential mechanism that results in reduced particle-settling velocities relative to the still-water particle-settling velocity; however, additional research is needed to explore this hypothesis.

Previous laboratory studies have identified instances where turbulence originating from shear at the bed (Kreplin and Eckelmann, 1979; Leeder, 1983; Wei and Willmarth, 1991) and on the lee side of bedforms (Bennett and Best, 1995) was positively skewed (net upward orientation). As observed in this study, the observed skewness resulted from shorter but higher-magnitude upward velocity fluctuations relative to downward velocity fluctuations and was capable of generating significant net-upwards momentum transfer (Wei and Willmarth, 1991). Since Bagnold (1966) first postulated an asymmetry in vertical flow fluctuations as a driver of sediment suspension, experimental data has loosely linked its genesis to the nature of the Kelvin–Helmholtz instabilities generated in the shear layer (Bennett and Best, 1995); however, a more precise description of its origin or its role in natural river hydrodynamics and sediment transport remains largely elusive (Leeder, 1983).

Other mechanisms inherent in bedform-wake turbulence, beyond producing a skewness in the distribution of vertical-velocity fluctuations, have been identified that may result in reduced sediment particle-settling rates. Studies on the motion of sand particles in turbulent flow (Stommel, 1949; Tooby *et al.*, 1977; Nielsen, 1984) have shown that sand-sized particles may become trapped within the vortex of the eddies composing the bedform wake. Logically, the particles trapped within the rotating flow volume in the eddy vortex would be swept preferentially in the mean direction of the eddy and, as the eddies typically have a substantial mean upward trajectory, the downward settling movement of the particles would be reversed or significantly reduced. This 'eddy-trapping' process has been used as an explanation for the high sediment concentrations associated with turbulent boils observed in rivers (Bijker *et al.*, 1976; Shugar *et al.*, 2010), although the mechanics of the process have not been well explored in river-like flow conditions.

Schmeeckle *et al*. (1999) and Venditti and Bennett (2000) describe mechanisms closely related to eddy trapping that occur during eddy genesis over bedforms. Using a combination of particle-imaging velocimetry and numerical modelling, Schmeeckle *et al*. (1999) describe two mechanisms that

Table 3. Predicted particle deposition values upon the model domain bed for each scenario

Scenario	% Particle feed deposited	% Change due to turbulence	Turbulence type simulated
Static velocity	86	–	none
Reference	65	−24.4[a]	bedform-generated and background
Flat bed, static velocity	49	–	none
Flat bed	45	−4.7[b]	background

[a]Relative to the 'static-vel.' scenario.
[b]Relative to the 'flat-bed, static-vel.' scenario.

contribute to the net upward flux of near-bed suspended sediment: (1) an expansion of the near-bed shear layer at a bedform crest preceding eddy development that sucks near-bed sediment upwards and (2) the inclusion of flow with relatively high sediment concentrations sourced from within the recirculation zone on the bedform lee side into the eddy structure during the eddy development and shedding process. In a laboratory experiment employing fixed acoustic Doppler velocimetry and optical turbidity sensors, Venditti and Bennett (2000) generally confirmed the results of Schmeeckle *et al.* (1999) and found that near-bed sediment launched higher into the flow column by bedform-generated turbulence accounted for nearly all of the sediment suspension occurring during their experiment.

Bradley *et al.* (2013) provide field evidence that dunes may promote locally high sediment transport concentrations without the production of a significant turbulent wake. In a study of low-angled dunes in the estuarine reach of the Fraser River, they found that vertical, topographically induced currents generated over the stoss-side slope of a dune were responsible for lifting significant fractions of near-bed sediment into the flow column and served as the source for up to 69% of the total suspended-sediment transport passing over the dune. In a similar field study of an estuarine reach of the Elba River, Kwoll *et al.* (2013) found that tides heavily modulated the influence of the turbulent wake on suspended-sediment transport. They report that, during tidally induced periods of slack water, low river velocities passing over bedforms did not generate adequate turbulence to influence suspended-sediment behaviour. As tides shifted and near-bed flow velocities accelerated, turbulence structures generated in the lee of bedforms became increasingly important drivers of total suspended-sediment transport flux. In the final stage, when the tidal conditions produced the maximum channel flow velocities, the influence of the bedform-generated turbulence on the suspended-sediment flux deteriorated as the influence of bed stress became the dominate driver.

Our numerical results show that particles are preferentially located within eddy structures and that the eddies are efficient at lifting near-bed sediment particles higher into the flow column. This phenomenon has been documented in the field for decades (e.g. Kostaschuk and Church, 1993); however, high-resolution illustration of the interaction between turbulence and suspended particles, as presented in our study, is rare. Figure 12 shows that in the downstream model domain, the upper flow column is predominantly populated with sediment particles lifted upwards from a near-bed position by the wake turbulence, evidenced by the preponderance of particles with negative mean settling velocities in that area.

As referenced in the Introduction, there has been considerable research on the effect of nonlinear drag force on particle settling. While this effect, which can impact sediment settling in isotropic (non-directional) turbulence, has primarily been investigated in well-constrained flow conditions numerically or in the laboratory (Nielsen, 1993; Brucato *et al.*, 1998; Fung, 1998; Fornari *et al.*, 2016), it has been hypothesized to have a significant impact on suspended sediment in rivers (Murray, 1970). To approximate the general magnitude of the nonlinear drag effect on particle settling in the hydrodynamic conditions simulated in this study, we performed a simple one-dimensional (1D) modelling experiment (fully described in the online Supporting Information). In our 1D experiment, we calculated particle settling using the same equations of particle movement as in our 3D model [Equations (1)–(10)] but with simplified flow velocity: horizontal flow was set to zero, while vertical flow velocity was approximated as a sine wave with zero mean value. We simulated a range of turbulent intensities by varying the amplitude and frequency of the sine wave in a manner similar to Murray (1970) and Stout *et al.* (1995). We found that for turbulence intensities in the range observed in the lower Mississippi River (McQuivey, 1973), the nonlinear drag effect may significantly reduce mean particle-settling velocities up to approximately 10%. However, the largest realistic turbulence intensities tested did not reduce particle-settling rates to the extent observed in our 3D modelling results, which suggests that mechanisms related to anisotropic turbulence have a far greater influence on sediment settling through bedform-generated turbulence.

Our study simulated turbulence generated from a bedform with a 14° lee-side slope angle. While we did not perform statistical tests to identify the frequency of the instances of predicted flow separation, qualitative observations suggest that a significant fraction of the flow separation occurring above the bedform lee-side slope was permanent. Field and laboratory observations (e.g. Kostaschuk and Villard, 1996; Best and Kostaschuk, 2002; Lefebvre *et al.*, 2014; Kwoll *et al.*, 2016) of flow over dunes suggest that permanent flow separation typically only occurs over the lee-side slope near the angle of repose (i.e. ~30°), although other numerical modelling studies (e.g. Paarlberg *et al.*, 2009; Lefebvre and Winter, 2016) have predicted that permanent flow separation may occur from dunes with lee-side slope angles between 10 and 20°. Research on dunes with variable lee-side slope angles typically suggests that smaller angles produce systematically smaller and more intermittent instances of separated flow (Best, 2005; Kwoll *et al.*, 2016).

Our numerical model simulated 3D flow, however, for simplicity, the bedform morphology incorporated into the model domain did not vary in the cross-stream dimension. The influence of 3D properties of dunes and dune fields on reach-scale flow, sediment transport, and channel morphology has been well documented in the field (e.g. Dietrich and Smith, 1984; Parsons *et al.*, 2005; Herbert and Alexander, 2018), laboratory (e.g. Venditti, 2007), and by numerical modelling (e.g. Johns and Xing, 1993; Omidyeganeh and Piomelli, 2013; Chen *et al.*, 2015). Of particular relevance to our study, Lefebvre (2019) used numerical modelling to show that the lateral orientation of the lee-side slope relative to the mean direction of the flow passing over the bedform is a primary control of the lee-side flow separation and turbulent wake production. Lefebvre (2019) found that as the lee-side slope became less perpendicular to the mean flow direction, flow separation was reduced. The exclusion of bedform three-dimensionality in our model should be considered when extrapolating our results to natural rivers.

This study focused on how bedform-generated turbulence impacts the settling of medium sand-sized particles. The settling behaviour of different particle size fractions may be substantially different than that identified by our study results. Medium sand settling was strongly sensitive to the range of bedform-generated turbulence simulated in our study. This sensitivity was likely promoted by the fact that, as medium sand particles settled from the outer flow column into the turbulent wake zone, the ratio of their W_S to the local turbulent intensity ($U_Z{}'_{RMS}$), which may serve as a criterion for transport mode (Raudkivi, 1998), became increasingly supportive of particle suspension (shifting from $W_S / U_Z{}'_{RMS} > 1$ to $W_S / U_Z{}'_{RMS} < 1$). Settling of particle-size fractions that do not experience a significant shift in their $W_S / U_Z{}'_{RMS}$ ratio upon contact with the wake zone, either maintaining consistent strong suspension ($W_S / U_Z{}'_{RMS} << 1$) or a lack of suspension ($W_S / U_Z{}'_{RMS} >> 1$), would be relatively insensitive to bedform-generated turbulence. Based on the range of turbulence intensities predicted for the bedform wakes in this study, the settling behaviour of particles smaller than fine sand (W_S for fine sand $= 0.01\,\mathrm{m\,s^{-1}}$)

or larger than very coarse sand (W_S for coarse sand = 0.15 m s^{-1}) would not likely be significantly impacted.

Implications for suspended-sediment concentrations and bedform dynamics

Our study illuminates how turbulence contributes to a reduction in sediment-settling rates, which may have a substantial effect on suspended-sediment transport and bedform dynamics. A general reduction in settling rates increases the time a particle of bed sediment will spend suspended in the flow column and, if particle entrainment processes are negligibly affected by the reduced settling (e.g. if there is no corresponding sediment-supply limitations or turbulence dampening) (VanSickle and Beschta, 1983; Sheng and Villaret, 1989), will result in higher suspended-sediment concentrations. While previous studies focusing on bedform-generated turbulence often identify higher concentrations of suspended sediment in the bedform-wake area (Lapointe, 1992; Kostaschuk and Church, 1993; Venditti and Bennett, 2000), the effect of bedforms on reach-scale suspended-sediment concentrations is less well understood as bedforms modify sediment transport by additional (sometimes offsetting) mechanisms, such as by increasing flow resistance (Smith and McLean, 1977; Naqshband *et al.*, 2014).

Increasing suspended-sediment transport over subaqueous dunes has typically been shown to flatten the dune morphology (Bridge and Best, 1988; Bennett *et al.*, 1998; Kostaschuk and Best, 2005; Hendershot *et al.*, 2016; Bradley and Venditti, 2019). This flattening may result from a reduction in the angle of the lee-side slopes and from a decreased relative contribution of bedload transport, which predominantly drives bedform growth and steepening (Simons *et al.*, 1965; Carling *et al.*, 2000; Jerolmack and Mohrig, 2005) to the overall sediment flux. When increased suspended-sediment transport is also associated with a significant increase in sediment transport capacity, apparent dune flattening may result from the transition to an upper-stage plane bed (Simons and Richardson, 1961). There are some contrasting observations from natural channels that identified a positive relationship between suspended-sediment transport and dune height (e.g. Allen, 1978; Gabel, 1993; Amsler and Schreider, 1999), but in those instances the increase in dune height resulted from amalgamation of multiple dunes (Best, 2005; Reesink and Bridge, 2007).

In the event that dune flattening is caused by reduced slope angles, it is generally assumed to produce less flow acceleration over the stoss-side slope (Nelson *et al.*, 1993) and a smaller zone of flow separation on the lee side of the dune (Best and Kostaschuk, 2002; Kwoll *et al.*, 2016), which results in a less intense turbulent wake. As suggested by this study, reduced wake intensity generally promotes faster particle settling and could potentially lead to decreased suspended-sediment transport rates within the bedform-wake zone. However, the impact of dune flattening on reach-scale suspended-sediment transport is less certain. Lefebvre and Winter (2016) show that the hydraulic roughness produced by bedforms is positively related to the lee-side slope angle and dune height relative to flow depth. Reduced roughness results in increased flow velocities that would promote increased suspended transport rates generally (Raudkivi, 1998).

A relatively explicit result of this study is that suspended-sediment particles passing over a bedform crest will, on average, contact the channel bed further downstream under the influence of turbulence than without it. In the context of a dune field, by increasing the area over which particles passing over a dune will contact the bed, turbulence 'diffuses' the contribution of those particles to a larger number of downstream dunes. In cases where the deposition of suspended sediment plays an integral part in the dune dynamics, this increase in mean settling trajectory length could ultimately lead to the diffusion of dune properties (e.g. flattening or increased wave length) and, as particles moving in suspension have higher average velocities than particles moving in contact with the bed, higher bedform translation velocities (Hand and Bartberger, 1988; Prent and Hickin, 2001; McElroy and Mohrig, 2009; Parsons and Best, 2013; Naqshband *et al.*, 2014). In cases where suspended sediment is not a significant driver of dune dynamics, increased trajectory lengths would lead to higher instances of particle 'bypassing' for individual dunes (Mohrig and Smith, 1996; Naqshband *et al.*, 2014). In the model of dune evolution postulated by Mohrig and Smith (1996), particles suspended over a dune crest must interact with the stoss-side slope of the downstream dune if that particle is going to contribute to the net translation of dunes within a field; particles bypassing the stoss-side slope contribute to the fraction of the sediment load not represented by the bedform sediment flux. Given the assumptions of that model, by increasing the settling trajectory length, bedform-generated turbulence decreases the overall flux of sediment transported in bedforms. It is logical to assume that, in cases where particles bypass one dune to contribute to another dune further downstream, the bypass would lead to decreased symmetry between neighbouring dunes rather than an overall reduction in bedform sediment flux.

Implications for suspended-sediment transport and morphological modelling

A common method to model suspended-sediment transport is to incorporate the Rouse number as a criterion for particle suspension. While initially developed to predict equilibrium sediment concentration profiles under uniform flow conditions over a flat-plane bed, models reliant on a Rouse number-type approach have been used to predict suspended-sediment transport in a range of dynamic hydrodynamic environments (Gelfenbaum and Smith, 1986). Our study provides additional evidence that the Rouse number is not necessarily applicable in the proximity of bedforms (Atkins *et al.*, 1989; Bennett *et al.*, 1998; Schmeeckle *et al.*, 1999). The Rouse number relies on the near-bed shear velocity ($u*$) as an estimate of the net-upwards vertical force balancing the downward pull of gravity on a particle (McLean, 1992; Leeder *et al.*, 2005); however, as shown in our study, the typically strong correlation between $u*$ and $U_Z{'}_{RMS}$ (Raudkivi, 1998) breaks down under the influence of bedform-wake turbulence (e.g. Figure 5). This lack of correlation derives from the fact that much of the bedform wake is generated from shear at the flow separation zone on the lee side of the bedform rather than shear at the bed, which may have a significantly different velocity distribution (Nelson *et al.*, 1995).

Due to the substantial effect of bedform-generated turbulence on sediment settling, morphodynamic models that disregard this effect may over-predict sediment deposition in the area downstream of the bedform and misrepresent sediment transport rates generally. As observed in our study, the presence of turbulent structures that significantly influence sediment settling and suspension may become unidentifiable in the mean flow field (Chang *et al.*, 2011). Suspended-sediment models based on temporal-averaged hydrodynamics and gradient diffusion would not resolve these turbulent structures or the relatively high loads of sediment transported within them. Further, models that do not fully resolve the key structures of the wake turbulence, such as the eddy dynamics (e.g. those that use turbulence statistics to incorporate the mean impact of turbulence, such as RANS-based models), may not accurately predict sediment deposition in the wake zone (Keylock *et al.*, 2014). This is because the properties of the discrete turbulence fluctuations, in terms of the fluctuation magnitudes and durations, have been shown to be substantially better correlated to the resultant sediment transport than the temporally averaged fluctuation values due to the highly nonlinear positive relationship between flow velocity and sediment flux (McLean *et al.*, 1994; Nelson *et al.*, 1995; Hurther and Lemmin, 2003; Bhaganagar and Hsu, 2009; Lelouvetel *et al.*, 2009; Schmeeckle, 2015). Recent research (e.g. Chang and Scotti, 2003; Tominaga and Stathopoulos, 2011; Keylock *et al.*, 2012; Alvarez *et al.*, 2017) has shown how turbulent-resolving models, such as those employing LES, more accurately predict flow and particulate transport than models reliant on turbulent statistics.

In geomorphic models of river systems, bedforms are often assumed to reduce suspended-sediment transport by adding roughness to the channel bed and decelerating the overall flow velocity (van Rijn, 1984; Garcia and Parker, 1991), despite a growing breadth of field evidence that suggests this assumption may not be universally applicable (Rood and Hickin, 1989; Kostaschuk and Church, 1993; Venditti and Bennett, 2000; Kostaschuk *et al.*, 2009; Bradley *et al.*, 2013). As suggested by our study, it is probable that due to the reduced settling in the bedform-wake zone, bedforms increase suspended sediment-transport rates locally in certain configurations. Studies of submerged vegetation (e.g. Yang, 2007; Ortiz *et al.*, 2013; Yager and Schmeeckle, 2013), which is also often regarded as a roughness element similar to dunes (Vargas-Luna *et al.*, 2015), have shown that it can promote sediment transport through the persistent generation of turbulence dependent on stem morphology and density (Nepf, 1999; Yang and Nepf, 2018).

Conclusions

Our study objective was to quantify bedform-generated turbulence influences on medium sand-sized particle settling in river-like flow conditions and assess how that influence might impact suspended-sediment and bedform dynamics. We used a numerical model to simulate 3D flow and suspended-particle fields to investigate sediment settling through the wake of a large, dune-scale bedform. To isolate the effect of turbulence on sediment settling, we simulated scenarios with and without temporally fluctuating flow. To differentiate the effect of the bedform wake on particle settling relative to that of background turbulence alone, we simulated scenarios with and without a bedform present on the channel bed.

On average, the presence of bedform-generated turbulence increased turbulence intensity within the model domain and generally reduced particle-settling velocities. Local values of particle-settling velocity and the settling trajectory of individual particles were significantly influenced by anisotrophic turbulent structures resolved within the flow-velocity field. Over the model domain, bedform-generated plus background turbulence reduced the settling velocity of suspended particles by approximately 50% relative to that estimated in flow without turbulent fluctuations. This reduction in settling velocity resulted in 24% fewer particles becoming deposited within the model domain. Background turbulence alone was calculated to have decreased settling velocity by up to 30% and decreased deposition within the domain by 5%. Our study examined a bedform with a relatively low lee-side slope angle (14°). Bedforms with larger angles near the angle of repose (~30°) would likely generate more intense wakes with a greater impact on particle settling.

The vertical-particle velocity was only significantly different than the vertical-flow velocity for very short time periods after high-magnitude fluctuations in the vertical-flow velocity. The mechanism by which turbulence reduced particle settling was attributed to the production of positively skewed vertical-velocity distributions. These distributions appeared to vary in space and were related to the mean turbulence intensity of the flow field.

The interplay between bedforms, the generation of turbulence, and sediment transport is complex, and the relative impact of the related individual processes is difficult to detangle from one another. Numerical modelling studies, such as this study, that can simulate synthetic scenarios designed to isolate the impact of processes and properties that cannot be isolated in the real world, in a realistic physics-driven manner, may be of great use to improve our scientific understanding. To simplify our study methodology, the basis of our analysis was a single, simplified bedform and we limited our investigation to the particle-settling process and explicitly did not simulate sediment-particle entrainment.

Acknowledgements—This study was funded by The Water Institute of the Gulf Science and Engineering Plan and the Louisiana Coastal Protection and Restoration Authority. Diana Di Leonardo helped improve the clarity of this manuscript. Luca Solari provided editorial support of a previous version of this manuscript that improved its quality.

Data Availability Statement

The data that support the findings of this study are available from the corresponding author upon reasonable request.

Conflict of Interest

The authors declare no conflict of interest.

References

Allen JRL. 1978. Polymodal dune assemblages: an interpretation in terms of dune creation—destruction in periodic flows. *Sedimentary Geology* **20**: 17–28.

Allison MA, Yuill BT, Meselhe EA, Marsh JK, Kolker AS, Ameen AD. 2017. Observational and numerical particle tracking to examine sediment dynamics in a Mississippi River delta diversion. *Estuarine, Coastal and Shelf Science* **194**: 97–108. https://doi.org/10.1016/j.ecss.2017.06.004

Alvarez LV, Schmeeckle MW, Grams PE. 2017. A detached eddy simulation model for the study of lateral separation zones along a large canyon-bound river. *Journal of Geophysical Research: Earth Surface* **122**: 25–49.

Amsler ML, Schreider MI. 1999. Dune height prediction at floods in the Paraná River, Argentina. In *River Sedimentation: Theory and Applications*, Jayewardena AW, Lee JHW, Wang ZY (eds). A.A. Balkema: Rotterdam; 615–620.

Atkins R, Soulsby RL, Waters CB, Oliver N. 1989. Field measurements of sediment suspension above bedforms in a sandy estuary. Technical Report. Hydraulics Research: Wallingford.

Badano ND, Sabarots Gerbec M, Re M, Menéndez AN. 2012. A coupled hydrosedimentologic model to assess the advance of the Parana River Delta Front. In *Proceedings of the Sixth International Conference on Fluvial Hydraulics, San Jose, Costa Rica*.

Bagnold RA. 1966. *An Approach to the Sediment Transport Problem from General Physics*. US Government Printing Office: Washington, D.C.

Bennett SJ, Best JL. 1995. Mean flow and turbulence structure over fixed, two-dimensional dunes: implications for sediment transport and bedform stability. *Sedimentology* **42**: 491–513. https://doi.org/10.1111/j.1365-3091.1995.tb00386.x

Bennett SJ, Bridge JS, Best JL. 1998. Fluid and sediment dynamics of upper stage plane beds. *Journal of Geophysical Research: Oceans* **103**: 1239–1274. https://doi.org/10.1029/97JC02764

Best J. 2005. The fluid dynamics of river dunes: a review and some future research directions. *Journal of Geophysical Research: Earth Surface* **110**: 1–21. https://doi.org/10.1029/2004JF000218

Best J, Kostaschuk R. 2002. An experimental study of turbulent flow over a low-angle dune. *Journal of Geophysical Research: Oceans* **107**: 18-1–18-19.

Bhaganagar K, Hsu T-J. 2009. Direct numerical simulations of flow over two-dimensional and three-dimensional ripples and implication to sediment transport: steady flow. *Coastal Engineering* **56**: 320–331. https://doi.org/10.1016/j.coastaleng.2008.09.010

Bijker EW, Van Hijum E, Vellinga P. 1976. Sand transport by waves. In *Coastal Engineering Proceedings*.

Bradley RW, Venditti JG. 2019. The growth of dunes in rivers. *Journal of Geophysical Research: Earth Surface* **124**: 548–566.

Bradley RW, Venditti JG, Kostaschuk RA, Church M, Hendershot M, Allison MA. 2013. Flow and sediment suspension events over low-angle dunes: Fraser Estuary, Canada. *Journal of Geophysical Research: Earth Surface* **118**: 1693–1709.

Bridge JS, Best JL. 1988. Flow, sediment transport and bedform dynamics over the transition from dunes to upper-stage plane beds: implications for the formation of planar laminae. *Sedimentology* **35**: 753–763.

Brucato A, Grisafi F, Montante G. 1998. Particle drag coefficients in turbulent fluids. *Chemical Engineering Science* **53**: 3295–3314.

Carling PA, Williams JJ, Golz E, Kelsey AD. 2000. The morphodynamics of fluvial sand dunes in the River Rhine, near Mainz, Germany. II. Hydrodynamics and sediment transport. *Sedimentology* **47**(1), 253–278.

Cellino M, Lemmin U. 2004. Influence of coherent flow structures on the dynamics of suspended sediment transport in open-channel flow. *Journal of Hydraulic Engineering* **130**: 1077–1088.

Chakrabarti A, Chen Q, Smith HD, Liu D. 2016. Large eddy simulation of unidirectional and wave flows through vegetation. *Journal of Engineering Mechanics* **142**: 1–8, 04016048.

Chang YS. 2004. Suspended sediment and hydrodynamics above mildly sloped long wave ripples. *Journal of Geophysical Research* **109**: 1–16. https://doi.org/10.1029/2003JC001900

Chang YS, Park Y-G. 2016. Suspension of sediment particles over a ripple due to turbulent convection under unsteady flow conditions. *Ocean Science Journal* **51**: 127–135. https://doi.org/10.1007/s12601-016-0011-2

Chang Y, Scotti A. 2003. Entrainment and suspension of sediments into a turbulent flow over ripples. *Journal of Turbulence* **4**: 1–22. https://doi.org/10.1088/1468-5248/4/1/019

Chang WY, Constantinescu G, Tsai WF, Lien HC. 2011. Coherent structure dynamics and sediment erosion mechanisms around an in-stream rectangular cylinder at low and moderate angles of attack. *Water Resources Research* **47**(W12532), 1–16. https://doi.org/10.1029/2011WR010586.

Chen X, Cardenas MB, Chen L. 2015. Three-dimensional versus two-dimensional bed form-induced hyporheic exchange. *Water Resources Research* **51**: 2923–2936.

Davies AG, Thorne PD. 2016. On the suspension of graded sediment by waves above ripples: inferences of convective and diffusive processes. *Continental Shelf Research* **112**: 46–67. https://doi.org/10.1016/j.csr.2015.10.006

Dietrich WE. 1982. Settling velocity of natural particles. *Water Resources Research* **18**: 1615–1626. https://doi.org/10.1029/WR018i006p01615

Dietrich WE, Smith JD. 1984. Bed load transport in a river meander. *Water Resources Research* **20**: 1355–1380.

Duan JG, Julien PY. 2010. Numerical simulation of meandering evolution. *Journal of Hydrology* **391**: 34–46.

Dubief Y, Delcayre F. 2000. On coherent-vortex identification in turbulence. *Journal of Turbulence* **1**: 1–22. https://doi.org/10.1088/1468-5248/1/1/011

Engelund F, Fredsøe J. 1976. A sediment transport model for straight alluvial channels. *Hydrology Research* **7**: 293–306.

Fornari W, Picano F, Brandt L. 2016. Sedimentation of finite-size spheres in quiescent and turbulent environments. *Journal of Fluid Mechanics* **788**: 640–669. https://doi.org/10.1017/jfm.2015.698

Fung JCH. 1998. Effect of nonlinear drag on the settling velocity of particles in homogeneous isotropic turbulence. *Journal of Geophysical Research: Oceans* **103**: 27905–27917. https://doi.org/10.1029/98JC02822

Gabel SL. 1993. Geometry and kinematics of dunes during steady and unsteady flows in the Calamus River, Nebraska, USA. *Sedimentology* **40**: 237–269.

Garcia M, Parker G. 1991. Entrainment of bed sediment into suspension. *Journal of Hydraulic Engineering* **117**: 414–435.

Gelfenbaum G, Smith JD. 1986. Experimental evaluation of a generalized suspended-sediment transport theory. In *Shelf Sands and Sandstones*, Knight RJ, McLean JR (eds). Canadian Society of Petroleum Geologists: Calgary; 133–134.

Grass AJ. 1971. Structural features of turbulent flow over smooth and rough boundaries. *Journal of Fluid Mechanics* **50**: 233–255.

Grigoriadis DGE, Balaras E, Dimas AA. 2009. Large-eddy simulations of unidirectional water flow over dunes. *Journal of Geophysical Research* **114**(F02022), 1–19. https://doi.org/10.1029/2008JF001014

Hand BM, Bartberger CE. 1988. Leeside sediment fallout patterns and the stability of angular bedforms. *Journal of Sedimentary Research* **58**: 33–43. https://doi.org/10.1306/212F8D05-2B24-11D7-8648000102C1865D

Hendershot ML, Venditti JG, Bradley RW, Kostaschuk RA, Church M, Allison MA. 2016. Response of low-angle dunes to variable flow. *Sedimentology* **63**: 743–760.

Herbert CM, Alexander J. 2018. Bottomset architecture formed in the troughs of dunes and unit bars. *Journal of Sedimentary Research* **88**: 522–553.

Howard AD. 1971. Simulation of stream networks by headword growth and branching. *Geographical Analysis* **3**: 29–50.

Hurther D, Lemmin U. 2003. Turbulent particle flux and momentum flux statistics in suspension flow. *Water Resources Research* **39**(5), 1139–1150. https://doi.org/10.1029/2001WR001113.

Jerolmack DJ, Mohrig D. 2005. A unified model for subaqueous bed form dynamics. *Water Resources Research* **41**(W12421), 1–10. https://doi.org/10.1029/2005WR004329.

Johannesson H, Parker G. 1989. Linear theory of river meanders. *River Meandering* **12**: 181–213.

Johns B, Xing J. 1993. Three-dimensional modelling of the free surface turbulent flow of water over a bedform. *Continental Shelf Research* **13**: 705–721.

Keylock CJ, Constantinescu G, Hardy RJ. 2012. The application of computational fluid dynamics to natural river channels: eddy resolving versus mean flow approaches. *Geomorphology* **179**: 1–20. https://doi.org/10.1016/j.geomorph.2012.09.006

Keylock CJ, Lane SN, Richards KS. 2014. Quadrant/octant sequencing and the role of coherent structures in bed load sediment entrainment. *Journal of Geophysical Research: Earth Surface* **119**: 264–286. https://doi.org/10.1002/2012JF002698

Khosronejad A, Sotiropoulos F. 2014. Numerical simulation of sand waves in a turbulent open channel flow. *Journal of Fluid Mechanics* **753**: 150–216. https://doi.org/10.1017/jfm.2014.335

Kirchner JW, Dietrich WE, Iseya F, Ikeda H. 1990. The variability of critical shear stress, friction angle, and grain protrusion in water-worked sediments. *Sedimentology* **37**: 647–672.

Kostaschuk R. 2000. A field study of turbulence and sediment dynamics over subaqueous dunes with flow separation. *Sedimentology* **47**: 519–531.

Kostaschuk R, Best J. 2005. Response of sand dunes to variations in tidal flow: Fraser Estuary. *Canada. Journal of Geophysical Research: Earth Surface* **110**(F04S04), 1–10. https://doi.org/10.1029/2004JF000176

Kostaschuk RA, Church MA. 1993. Macroturbulence generated by dunes: Fraser River, Canada. *Sedimentary Geology* **85**: 25–37. https://doi.org/10.1016/0037-0738(93)90073-E

Kostaschuk R, Villard P. 1996. Flow and sediment transport over large subaqueous dunes: Fraser River, Canada. *Sedimentology* **43**: 849–863.

Kostaschuk RA, Villard PV. 1999. Turbulent sand suspension over dunes. In *Fluvial Sedimentology VI*, Vol. **28**; 3–14.

Kostaschuk R, Shugar D, Best J, Parsons D, Lane S, Hardy R, Orfeo O. 2009. Suspended sediment transport and deposition over a dune: Río Paraná, Argentina. *Earth Surface Processes and Landforms* **34**: 1605–1611.

Kreplin H-P, Eckelmann H. 1979. Behavior of the three fluctuating velocity components in the wall region of a turbulent channel flow. *The Physics of Fluids* **22**: 1233–1239.

Kwoll E, Winter C, Becker M. 2013. Intermittent suspension and transport of fine sediment over natural tidal bedforms. In *Coherent Flow Structures at Earth's Surface*, Venditti JG, Best JL, Church M, Hardy RJ (eds). Wiley-Blackwell: Oxford; 231–242.

Kwoll E, Venditti JG, Bradley RW, Winter C. 2016. Flow structure and resistance over subaqueous high- and low-angle dunes. *Journal of Geophysical Research: Earth Surface* **121**: 545–564. https://doi.org/10.1002/2015JF003637

Lai YG, Bandrowski DJ. 2014. Large wood flow hydraulics: a 3D modelling approach. In *Proceedings of Bold Visions for Environmental Modelling, San Diego, CA*.

Lapointe M. 1992. Burst-like sediment suspension events in a sand bed river. *Earth Surface Processes and Landforms* **17**: 253–270. https://doi.org/10.1002/esp.3290170305

Leeder MR. 1983. On the dynamics of sediment suspension by residual Reynolds stresses—confirmation of Bagnold's theory. *Sedimentology* **30**: 485–491.

Leeder MR, Gray TE, Alexander J. 2005. Sediment suspension dynamics and a new criterion for the maintenance of turbulent suspensions. *Sedimentology* **52**: 683–691.

Lefebvre A. 2019. Three-dimensional flow above river bedforms: insights from numerical modeling of a natural dune field (Río Paraná, Argentina). *Journal of Geophysical Research: Earth Surface* **124**: 2241–2264.

Lefebvre A, Winter C. 2016. Predicting bed form roughness: the influence of lee side angle. *Geo-Marine Letters* **36**: 121–133.

Lefebvre A, Paarlberg AJ, Winter C. 2014. Flow separation and shear stress over angle-of-repose bed forms: a numerical investigation. *Water Resources Research* **50**: 986–1005. https://doi.org/10.1002/2013WR014587

Lelouvetel J, Bigillon F, Doppler D, Vinkovic I, Champagne J-Y. 2009. Experimental investigation of ejections and sweeps involved in particle suspension. *Water Resources Research* **45**(W02416), 1–15. https://doi.org/10.1029/2007WR006520

Luchik TS, Tiederman WG. 1987. Timescale and structure of ejections and bursts in turbulent channel flows. *Journal of Fluid Mechanics* **174**: 529–552.

Marchioli C, Armenio V, Salvetti MV, Soldati A. 2006. Mechanisms for deposition and resuspension of heavy particles in turbulent flow over wavy interfaces. *Physics of Fluids* **18**: 1–16, 025102. https://doi.org/10.1063/1.2166453

McElroy B, Mohrig D. 2009. Nature of deformation of sandy bed forms. *Journal of Geophysical Research* **114**(F00A04), 1–13. https://doi.org/10.1029/2008JF001220

McLean SR. 1992. On the calculation of suspended load for noncohesive sediments. *Journal of Geophysical Research: Oceans* **97**: 5759–5770.

McLean SR, Nelson JM, Wolfe SR. 1994. Turbulence structure over two-dimensional bed forms: implications for sediment transport. *Journal of Geophysical Research* **99**(C6), 12729–12747. https://doi.org/10.1029/94JC00571

McQuivey RS. 1973. *Summary of Turbulence Data from Rivers, Conveyance Channels, and Laboratory Flumes: Turbulence in Water*. US Government Printing Office: Washington, D.C.

Middleton GV, Southard JB. 1984. *Mechanics of sediment movement*. Short Course No. 3. Society of Economic Paleontologists and Mineralogists: Providence, RI.

Mohrig D, Smith JD. 1996. Predicting the migration rates of subaqueous dunes. *Water Resources Research* **32**: 3207–3217. https://doi.org/10.1029/96WR01129

Molinas A, Wu B. 2001. Transport of sediment in large sand-bed rivers. *Journal of Hydraulic Research* **39**: 135–146.

Müller A, Gyr A. 1986. On the vortex formation in the mixing layer behind dunes. *Journal of Hydraulic Research* **24**: 359–375.

Murray SP. 1970. Settling velocities and vertical diffusion of particles in turbulent water. *Journal of Geophysical Research* **75**: 1647–1654. https://doi.org/10.1029/JC075i009p01647

Murray AB, Paola C. 1994. A cellular model of braided rivers. *Nature* **371**: 54–57.

Nagata N, Hosoda T, Muramoto Y. 2000. Numerical analysis of river channel processes with bank erosion. *Journal of Hydraulic Engineering* **126**: 243–252.

Naqshband S, Ribberink JS, Hurther D, Hulscher SJ. 2014. Bed load and suspended load contributions to migrating sand dunes in equilibrium. *Journal of Geophysical Research: Earth Surface* **119**: 1043–1063.

Nelson JM, McLean SR, Wolfe SR. 1993. Mean flow and turbulence fields over two-dimensional bed forms. *Water Resources Research* **29**: 3935–3953. https://doi.org/10.1029/93WR01932

Nelson JM, Shreve RL, McLean SR, Drake TG. 1995. Role of near-bed turbulence structure in bed load transport and bed form mechanics. *Water Resources Research* **31**: 2071–2086. https://doi.org/10.1029/95WR00976

Nepf HM. 1999. Drag, turbulence, and diffusion in flow through emergent vegetation. *Water Resources Research* **35**: 479–489.

Nielsen P. 1984. On the motion of suspended sand particles. *Journal of Geophysical Research: Oceans* **89**: 616–626.

Nielsen P. 1993. Turbulence effects on the settling of suspended particles. *SEPM Journal of Sedimentary Research* **63**(5), 835–838. https://doi.org/10.1306/D4267C1C-2B26-11D7-8648000102C1865D

Nittrouer JA, Allison MA, Campanella R. 2008. Bedform transport rates for the lowermost Mississippi River. *Journal of Geophysical Research* **113**(F03004), 1–16. https://doi.org/10.1029/2007JF000795

Omidyeganeh M, Piomelli U. 2013. Large-eddy simulation of three-dimensional dunes in a steady, unidirectional flow. Part 2. Flow structures. *Journal of Fluid Mechanics* **734**: 509–534.

Ortiz AC, Ashton A, Nepf H. 2013. Mean and turbulent velocity fields near rigid and flexible plants and the implications for deposition. *Journal of Geophysical Research: Earth Surface* **118**: 2585–2599.

Paarlberg AJ, Dohmen-Janssen CM, Hulscher SJ, Termes P. 2009. Modeling river dune evolution using a parameterization of flow separation. *Journal of Geophysical Research: Earth Surface* **114**(F01014), 1–17. https://doi.org/10.1029/2007JF000910

Paola C, Twilley RR, Edmonds DA, Kim W, Mohrig D, Parker G, Viparelli E, Voller VR. 2011. Natural processes in delta restoration: application to the Mississippi Delta. *Annual Review of Marine Science* **3**: 67–91. https://doi.org/10.1146/annurev-marine-120709-142856

Papanicolaou AN, Diplas P, Evaggelopoulos N, Fotopoulos S. 2002. Stochastic incipient motion criterion for spheres under various bed packing conditions. *Journal of Hydraulic Engineering* **128**: 369–380.

Parsons DR, Best J. 2013. Bedforms: views and new perspectives from the Third International Workshop on Marine and River Dune Dynamics (MARID3). *Earth Surface Processes and Landforms* **38**: 319–329.

Parsons DR, Best JL, Orfeo O, Hardy RJ, Kostaschuk R, Lane SN. 2005. Morphology and flow fields of three-dimensional dunes, Rio Paraná, Argentina: results from simultaneous multibeam echo sounding and acoustic Doppler current profiling. *Journal of Geophysical Research: Earth Surface* **110**(F04S03), 1–9. https://doi.org/10.1029/2004JF000231

Pasiok R, Stilger-Szydło E. 2010. Sediment particles and turbulent flow simulation around bridge piers. *Archives of Civil and Mechanical Engineering* **10**: 67–79.

Prent MT, Hickin EJ. 2001. Annual regime of bedforms, roughness and flow resistance, Lillooet River, British Columbia, BC. *Geomorphology* **41**: 369–390.

Ramirez MT, Allison MA. 2013. Suspension of bed material over sand bars in the Lower Mississippi River and its implications for Mississippi delta environmental restoration. *Journal of Geophysical Research: Earth Surface* **118**: 1085–1104. https://doi.org/10.1002/jgrf.20075

Raudkivi AJ. 1998. *Loose Boundary Hydraulics*. A.A. Balkema: Rotterdam.

Reesink AJH, Bridge JS. 2007. Influence of superimposed bedforms and flow unsteadiness on formation of cross strata in dunes and unit bars. *Sedimentary Geology* **202**: 281–296.

van Rijn LC. 1984. Sediment transport, part II: suspended load transport. *Journal of Hydraulic Engineering* **110**: 1613–1641.

van Rijn LC. 2007. Unified view of sediment transport by currents and waves. II: Suspended Transport. *Journal of Hydraulic Engineering* **133**: 668–689. https://doi.org/10.1061/(ASCE)0733-9429(2007)133:6(668)

van Rijn LC, Tan GL. 1985. SUTRENCH-model: two-dimensional vertical mathematical model for sedimentation in dredged channels and trenches by currents and waves. Rijkswaterstaat Communications: The Hague.

Rood KM, Hickin EJ. 1989. Suspended-sediment concentration and calibre in relation to surface-flow structure in Squamish River estuary, southwestern British Columbia. *Canadian Journal of Earth Sciences* **26**: 2172–2176. https://doi.org/10.1139/e89-183

Schmeeckle MW. 2014. Numerical simulation of turbulence and sediment transport of medium sand. *Journal of Geophysical Research: Earth Surface* **119**: 1240–1262.

Schmeeckle MW. 2015. The role of velocity, pressure, and bed stress fluctuations in bed load transport over bed forms: numerical simulation downstream of a backward-facing step. *Earth Surface Dynamics* **3**: 105–112. https://doi.org/10.5194/esurf-3-105-2015

Schmeeckle MW, Shimizu Y, Hoshi K, Baba H, Ikezaki S. 1999. Turbulent structures and suspended sediment over two-dimensional dunes. *Journal of Hydraulic Engineering* **134**: 261–270.

Shams M, Ahmadi G, Smith DH. 2002. Computational modeling of flow and sediment transport and deposition in meandering rivers. *Advances in Water Resources* **25**: 689–699.

Sheng YP, Villaret C. 1989. Modeling the effect of suspended sediment stratification on bottom exchange processes. *Journal of Geophysical Research: Oceans* **94**: 14429–14444.

Shugar DH, Kostaschuk R, Best JL, Parsons DR, Lane SN, Orfeo O, Hardy RJ. 2010. On the relationship between flow and suspended sediment transport over the crest of a sand dune, Río Paraná, Argentina. *Sedimentology* **57**: 252–272.

Simons DB, Richardson EV. 1961. Forms of bed roughness in alluvial channel. *Journal of the Hydraulics Division* **87**: 87–105.

Simons DB, Richardson EV, Nordin Jr CF. 1965. Bedload Equation for Ripples and Dunes. U.S. Geological Survey Professional Paper: Washington, D.C.

Smith JD, McLean SR. 1977. Spatially averaged flow over a wavy surface. *Journal of Geophysical Research* **82**: 1735–1746.

Spalart P, Allmaras S. 1994. A one-equation turbulence model for aerodynamic flows. *La Recherche Aerospatiale* **1**: 5–21.

Stommel H. 1949. Trajectories of small bodies sinking slowly through convection cells. *Journal of Marine Research* **8**: 24–29.

Stout JE, Arya SP, Genikhovich EL. 1995. The effect of nonlinear drag on the motion and settling velocity of heavy particles. *Journal of the Atmospheric Sciences* **52**: 3836–3848. https://doi.org/10.1175/1520-0469(1995)052<3836:TEONDO>2.0.CO;2

Tominaga Y, Stathopoulos T. 2011. CFD modeling of pollution dispersion in a street canyon: comparison between LES and RANS. *Journal of Wind Engineering and Industrial Aerodynamics* **99**: 340–348.

Tooby PF, Wick GL, Isaacs JD. 1977. The motion of a small sphere in a rotating velocity field: a possible mechanism for suspending particles in turbulence. *Journal of Geophysical Research* **82**: 2096–2100.

Umlauf L, Burchard H. 2003. A generic length-scale equation for geophysical turbulence models. *Journal of Marine Research* **61**: 235–265. https://doi.org/10.1357/002224003322005087

VanSickle J, Beschta RL. 1983. Supply-based models of suspended sediment transport in streams. *Water Resources Research* **19**: 768–778.

Vargas-Luna A, Crosato A, Uijttewaal WS. 2015. Effects of vegetation on flow and sediment transport: comparative analyses and validation of predicting models. *Earth Surface Processes and Landforms* **40**: 157–176.

Venditti JG. 2007. Turbulent flow and drag over fixed two- and three-dimensional dunes. *Journal of Geophysical Research* **112** (F04008), 1–21. https://doi.org/10.1029/2006JF000650

Venditti JG, Bauer BO. 2005. Turbulent flow over a dune: Green River, Colorado. *Earth Surface Processes and Landforms: The Journal of the British Geomorphological Research Group* **30**: 289–304.

Venditti JG, Bennett SJ. 2000. Spectral analysis of turbulent flow and suspended sediment transport over fixed dunes. *Journal of Geophysical Research: Oceans* **105**: 22035–22047. https://doi.org/10.1029/2000JC900094

Wang Y. 2013. Development of a numerical tool to predict hydrodynamics, temperature and TDG in hydropower flows. PhD thesis, University of Iowa, Ames, IA.

Wang L-P, Maxey MR. 1993. Settling velocity and concentration distribution of heavy particles in homogeneous isotropic turbulence. *Journal of Fluid Mechanics* **256**: 27–68. https://doi.org/10.1017/S0022112093002708

Wang Y, Politano M, Laughery R, Weber L. 2015. Model development in OpenFOAM to predict spillway jet regimes. *Journal of Applied Water Engineering and Research* **3**: 80–94.

Wei T, Willmarth WW. 1991. Examination of v-velocity fluctuations in a turbulent channel flow in the context of sediment transport. *Journal of Fluid Mechanics* **223**: 241–252.

Wren DG, Kuhnle RA, Wilson CG. 2007. Measurements of the relationship between turbulence and sediment in suspension over mobile sand dunes in a laboratory flume. *Journal of Geophysical Research: Earth Surface* **112**(F03009), 1–14.

Yager EM, Schmeeckle MW. 2013. The influence of vegetation on turbulence and bed load transport. *Journal of Geophysical Research: Earth Surface* **118**: 1585–1601.

Yang S-Q. 2007. Turbulent transfer mechanism in sediment-laden flow. *Journal of Geophysical Research* **112**(F01005), 1–14. https://doi.org/10.1029/2005JF000452

Yang JQ, Nepf HM. 2018. A turbulence-based bed-load transport model for bare and vegetated channels. *Geophysical Research Letters* **45**: 10428–10436.

Zedler EA, Street RL. 2001. Large-eddy simulation of sediment transport: currents over ripples. *Journal of Hydraulic Engineering* **127**: 444–452. https://doi.org/10.1061/(ASCE)0733-9429(2001)127:6(444)

Zhao T, Dai F, Xu N. 2017. Coupled DEM-CFD investigation on the formation of landslide dams in narrow rivers. *Landslides* **14**: 189–201.[1]

Supporting Information

Additional supporting information may be found online in the Supporting Information section at the end of the article.

Supporting Information S1

[1]Std. dev. = standard deviation

